NTNU – Trondheim
Norwegian University of
Science and Technology

Navigated Ultrasound Imaging

3D Reconstruction of Artery Geometry and
Flow

Yücel Karabiyik

Medical Technology
Submission date: July 2013
Supervisor: Ilangko Balasingham, IET
Co-supervisor: Lasse Løvstakken, ISB

Norwegian University of Science and Technology
Department of Electronics and Telecommunications

Abstract

Atherosclerosis is a disease in which plaque builds up inside the arteries and causes the arteries to harden and narrow. The diagnosis of atherosclerosis and quantification of the extent of atherosclerosis nowadays depend on conventional two-dimensional (2D) images of the arteries while the plaque progression is in three-dimensions. The main objectives of this thesis are to develop an application software that can realize three-dimensional (3D) reconstructions of geometry and blood flow of arteries by using 2D ultrasound images and to evaluate the accuracy of the developed application. The method used for reconstruction is free-hand 3D ultrasound imaging with an optical tracker method. The Visualization Toolkit, which is a C++ class library for 3D computer graphics, and Qt which is a framework for creating graphical user interfaces, are utilized to develop the application.

In vivo and in vitro experiments are conducted for evaluation and the results of the experiments and sample 3D reconstructions are presented in the report. The spatial positioning accuracy of the application is found to be 0.36 mm RMS.

Acknowledgments

I am deeply grateful to Lasse Løvstakken for his constant support and the ideas that shaped this work. I would like to express my gratitude to Gabriel Kiss for his help with the problems I encountered throughout the development of the application. I also would like to thank Daniel Høyer Iversen for his generous support.

Contents

Part I
Introduction

This report presents the implementation and validation of an application software that can be used for three-dimensional (3D) reconstruction of geometry and blood flow of central and peripheral arteries, specifically the carotid arteries.

Reconstruction is done with free-hand 3D imaging with optical tracker method by utilizing a navigation system that is based on highly accurate optical sensors.

Part I of the report presents the objectives and motivation for this particular project. Part II provides the background to understand the aims and results of the project. Part III presents the software tools and equipment followed by the description of methods employed in this project. Part IV gives the methods used for in vivo and in vitro tests which are performed for validation of the application software. Part V presents the implementation and validation results. Results of the validation experiments are interpreted and discussed in Part VI. Finally, Part VII concludes the report and presents the recommendations for further work.

1 Ultrasound Imaging of Arteries and Diagnosis of Atherosclerosis

Plaques in the arteries is the main cause of the majority of myocardial infraction and ischemic strokes [18]. Due to an excessive build up of plaque around the artery wall, it becomes narrowed and hardened which disrupts the flow of blood within the body and can result in life-threatening conditions [21]. Therefore, diagnosis of atherosclerosis and quantification of its extent is of great value for risk stratification, evaluation of patient response to medical interventions and evaluation of new risk factors [19, 18]

Traditional two-dimensional (2D) ultrasound has been convenient for assessments of plaque progression, morphology and composition however, pathology related to atherosclerosis is essentially three-dimensional (3D). Accurate assessment of plaque changes with 2D ultrasound is difficult due to the variability in the conventional 2D ultrasound examination [19, 18]. It is difficult for clinicians to localize 2D ultrasound images in the body, therefore detailed assessment of plaque changes is challenging.

However, 3D ultrasound can allow quantitative monitoring of plaque volume

changes. Since plaque progression is in three directions, measurement of plaque volume has the potential to be more informative and sensitive than plaque area that is measured with 2D ultrasound [19].

Although, 3D echocardiography in particular give clinically important images, display of 3D ultrasound data of peripheral and central arteries has not yet received its due attention[8]. 3D transducers for vascular imaging are still not available.

2 Main objectives

As Section 1 points out, 3D ultrasound imaging improves the quality of diagnosis of vascular diseases, however 3D reconstruction of geometry and flow of arteries is still an area that needs be advanced.

This aims of this projects are

- to develop a software application that can realize 3D reconstruction of geometry and blod flow of arteries by using 2D ultrasound images and incorporating electrocardiogram signals
- to evaluate the accuracy of the developed application and the quality of the 3D reconstructions.

Part II
Theory and Background

3 Development of Ultrasound Imaging

The idea of using ultrasound technology in medical field was introduced in the late 1940's, after World War II. Radio Detection And Ranging (RADAR) and Sound Navigation And Ranging (SONAR) technologies that were developed during the war paved the way for using ultrasound as an imaging modality [1]. This imaging method is based on transmitting ultrasound waves towards a biological tissue and studying the back scattered waves. Scattered waves convey information about structure of the biological tissue. This method is very similar to working principle of RADAR and SONAR. Many terminologies were imported from these technologies [29].

Development of processing units, display technologies and integrated circuits enabled ultrasound systems to be complex and cutting-edge equipments of today.

During 1980s, transducer technology evolved tremendously. Specialized phased and linear arrays were developed for specific clinical applications such as cardiology, obstetrics/gynecology, surgical and vascular. Also during this period, many signal processing methods for imaging and calculations were developed [30].

In 1990s, developments in powerful microprocessors and low-cost analog/digital (A/D) chips allowed greater computation and faster processing in smaller volumes and at lower costs. Imaging systems, as a result, evolved into digital architectures. Also in this period, near-real-time[1] 3D imaging became possible [30]. True real-time 3D imaging with 2D array is more challenging since it involves hundreds of elements in the array and adequate number of channels to process the data and form the image. An early 2D array, 3D real-time imaging system was developed at Duke University in 1987 [30]. 3D imaging is still a challenge due to real time processing and visualization of large amount of data [1]. There are different methods for 3D imaging to avoid these problems which will be explained in the following chapters.

Nowadays, many advantages of ultrasound imaging allowed it to be one of the most widely used imaging technique in medicine [29]. It is portable, free

[1] term implies that there is a time delay, which is not significant, between occurrence and display

of radiation risk and relatively inexpensive when compared to other imaging modalities, such as magnetic resonance (MR) and computed tomography (CT).

4 Ultrasound Imaging Basics

Modern medical ultrasound imaging is performed in almost the same way as it was performed several decades ago. The basic method is pulse-echo approach with a brightness-mode (B-mode) display. Pulse-echo technique uses short pulses of ultrasound to construct 2D cross-sectional images. A transducer[2] transmits pulses into the patient's body for a very short period of time and after the transmission is complete, it listens to the reflected echoes. So the transducer works as a speaker (generates the sound waves) and a microphone (receives the sound waves). The ultrasound pulse consists of wave cycles that travel together. This technique is based on a technology known as Echo Ranging which is also basis of SONAR.

A pulsed ultrasound wave that is transmitted in the body hits an interface (acoustic mismatch between two media) and is partially reflected to the transducer. These reflected waves arising from different acoustic mismatches result in ultrasonic detection of interfaces within the body.

If the velocity of ultrasound in the medium and the elapsed time from the firing of the pulse are known, then the distance to an interface is calculated with the following formula

$$z = ct \tag{1}$$

where c is the velocity of the sound in the medium and t is the time of flight[15].

[2]"In ultrasound, a piezoelectric crystal converts an electrical stimulus into an ultrasound pulse and returning echo into an electric signal" [15]. In this report *transducer* may refer also to the probe of an ultrasound scanner. The reader may distinguish the difference from the context.

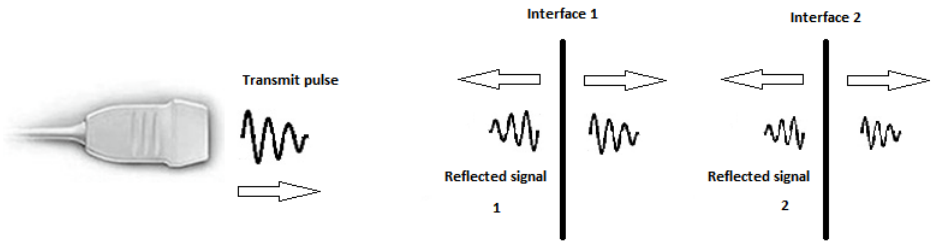

Figure 1: Basic ultrasound imaging principle

5 B-mode (2D Mode) Imaging

In B-mode imaging the amplitude of the reflected signal is represented by the brightness of a dot in the image. The position of the dot represents the depth which is calculated from (1). In order to create a 2D image, compound B-scanning is used, where multiple sets of dots are combined to picture the echo pattern from internal structures within the body.

A pulsed-wave, narrow ultrasound beam is directed along a straight-line path. After the echoes arrive to the transducer, the beam is directed along another path. Changing the direction of the beam is done mechanically or electronically in a repetitive and automated fashion. Therefore, a single image is constructed by sweeping pulsed beams along different sampling directions throughout the field of view (FOV)[3]. For each sampling direction, the amplitude of the back-scattered signal is coded in a gray scale and displayed. The process for single image is repeated to produce successive images of a region [15].

An example of B-mode image is give in Figure 2. Brighter areas correspond to higher amplitudes in the back-scattered signal.

[3]The physical region that is being imaged.

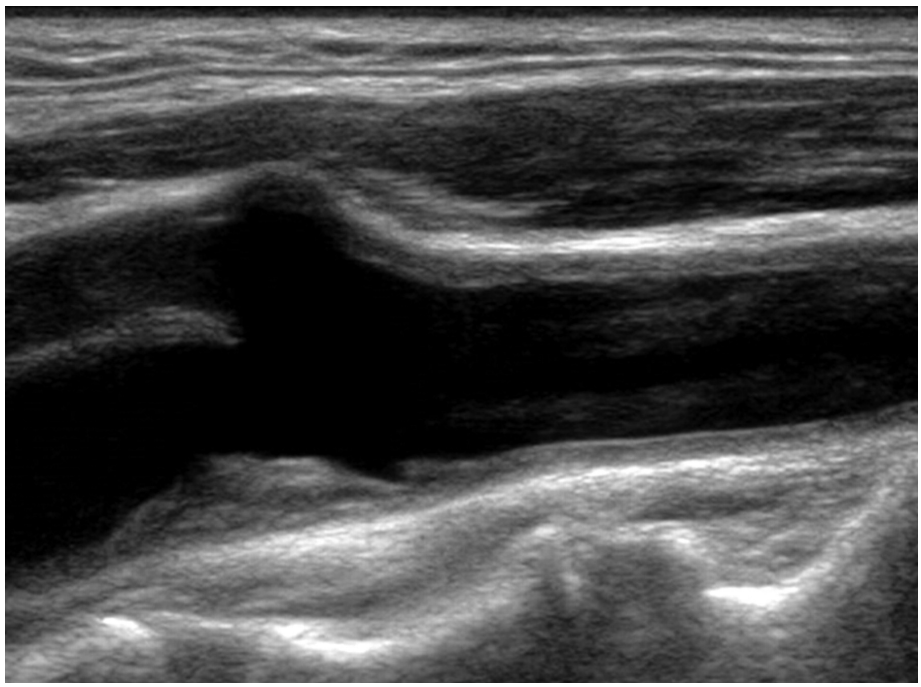

Figure 2: B-mode ultrasound image of carotid artery [22]

6 Color Flow Imaging

Color flow imaging (CFI), also known as color Doppler imaging, is an imaging method that combines anatomical information acquired using ultrasonic pulse-echo techniques with velocity information acquired using ultrasonic Doppler techniques to create color-coded maps of tissue velocity superimposed on gray-scale images of tissue anatomy[9]. The most common use of this method is the visualization and measurement of blood flow through the heart, arteries and veins [9, 31].

CFI techniques are similar to pulse-echo techniques in which information regarding the location of each target in the body, corresponding to each pixel in the image, is derived in the same way by using (1) for pulse round-trip transit time, but the returning echoes are analyzed in terms of frequency shift rather than amplitude [9]. This frequency change is due to the movement of

the scatterers, such as a cardiac wall or the blood. The frequency of the back scattered signal is different from the frequency of transmitted signal and this effect is called **Doppler effect** [1].

Doppler shift determines the color displayed at each point in the color image and by convention, red colors are used when flow is towards the probe and blue when flow is away from the probe. The color bar in Figure 3 shows a color range to indicate the amount of Doppler shift, ranging from dark shades of red and blue for low velocities to lighter shades for high velocities. Areas where flow is absent or too slow to be detected are black [12].

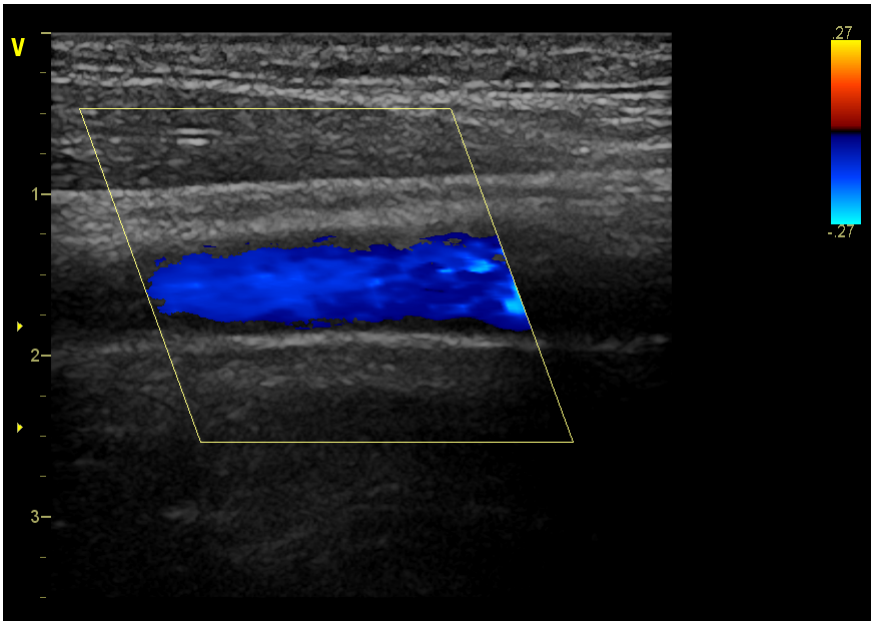

Figure 3: Color flow image of the carotid artery acquired with GE 11L linear probe

7 3D Imaging

7.1 Why 3D Imaging?

2D images can be acquired with conventional B-mode imaging for the area of interest in the body. Traditional B-mode ultrasound examination is a process which a clinician places the probe of an ultrasound scanner on subject's body and acquires 2D image of the cross-section of the body below the probe [11]. In this technique, clinician must mentally integrate the image in 3D anatomy of the body. In order to do this, the clinician must be trained and this process takes a great deal of time and requires intensive level of training [7].

On the other hand, 3D ultrasound imaging provides the whole volume of the area of interest, instead of only one slice 2D image. This allows the clinician to view and analyze the acquired data in various ways. The main advantages of 3D ultrasound over 2D ultrasound can be listed as follows:

• *Volume Measurements*

Linear dimension and cross-sectional area of the desired part of the body can be measured from a 2D view, however volume, which can be seen as crucial parameter, cannot be determined accurately. In 2D imaging, estimated volume and observed area relation depends on gross assumptions [16]

• *Extended 2D imaging capability*

Once the 3D data is acquired, clinician can take 2D slices that are impossible to obtain with 2D ultrasound. For example, a slice parallel to skin surface can be visualized with 3D imaging.

• *Optimal selection of 2D images*

In the process of diagnosis, it is often the case that a trained sonographer acquire one or more 2D image slices which are later examined by a qualified radiologist to make the diagnosis. As a result, diagnosis depends on the sonographer's skills to acquire the clinically most important view. In case the radiologist is not satisfied with the images, the patient may be called in for another examination. This causes inconvenience, delay and unnecessary cost. To avoid such incidents, the sonographer may acquire 3D volume of the area of interest so later the radiologist would navigate through this volume data and find the most significant views for diagnosis.

• *Intuitive interpretation*

As mentioned before, 2D images are not easy to interpret, particularly for users who are not experienced in viewing B-mode images. 3D images are more informative. These images may also be used in surgical planning. Surgeon may feel more confident depending on 3D image rather than his own interpretation

of a set of 2D cross-sections [16].

7.2 3D Ultrasound Data Acquisition Methods

Various techniques have been developed for acquisition of 3D ultrasound data. Most of the methods employ a 1D conventional probe and 2D images are taken by sweeping the probe over the area of interest on the patient's body. After acquisition acquisition of images, reconstruction is done by stacking up B-mode images to form a 3D image. To be able to reconstruct a 3D image volume without distortions, following three factors must be optimized [10]:

• Method that is being used must be either rapid or gated to avoid distortions from involuntary respiratory or cardiac motion.

• Position and orientation of 2D images that are acquired must be known precisely to avoid geometric deformation in the reconstructed volume. Geometric deformation may lead to measurement errors.

• The scanning apparatus should be simple and convenient to use so that the scanning process can be carried out easily.

Several 3D ultrasound imaging approaches have been developed to overcome the limitations of 2D imaging that are explained in Section 7.1 and optimize the factors mentioned above. These existing methods are reviewed briefly below.

7.2.1 Mechanical Swept Volume

Mechanical swept volume or motorized movement approach employs a motor inside the probe to sweep the plane of B-scan through volume of interest. Different methods use different sweep patterns therefore use different procedures to determine the position of each 2D image [11]. Nomenclature of imaging directions is given in Figure 4. It is necessary to understand the directions to be able to interpret this scanning approach.

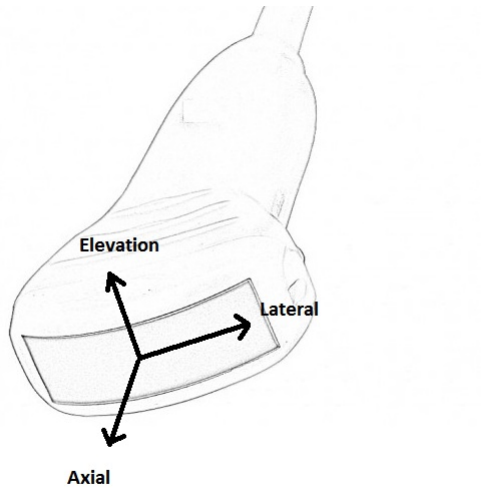

Figure 4: Imaging directions

Mechanical swept volume approach limits the movement of the probe to avoid distortion. Therefore, during the acquisition of data, the position of the probe must be kept fixed relative to the patient. The size of the measured volume is determined by the area of B-scan images [27]. Different types of scanning methods are explained below:

- ***Tilt scanning***

In this method, the probe is rotated about an axis in the lateral direction. This produces a fan-shaped volume. As can be seen from the Figure 5(a) the distance between the planes increases with the distance from the probe. This reduces the resolution of 3D volume with depth.

- ***Rotational scanning***

In this method, the probe is rotated about an axis in the axial direction. It results of in a cone shaped swept volume as shown Figure 5(b). However, it is crucial to keep the probe stable as in other mechanical approaches to get the best result.

- ***Linear scanning***

In this method, the probe is is moved mechanically through the area of interest along an axis in the elevation direction. Therefore, acquired images are parallel to each other with equal spacing. The result of this method is prism shaped swept volume as shown in Figure 5(c).

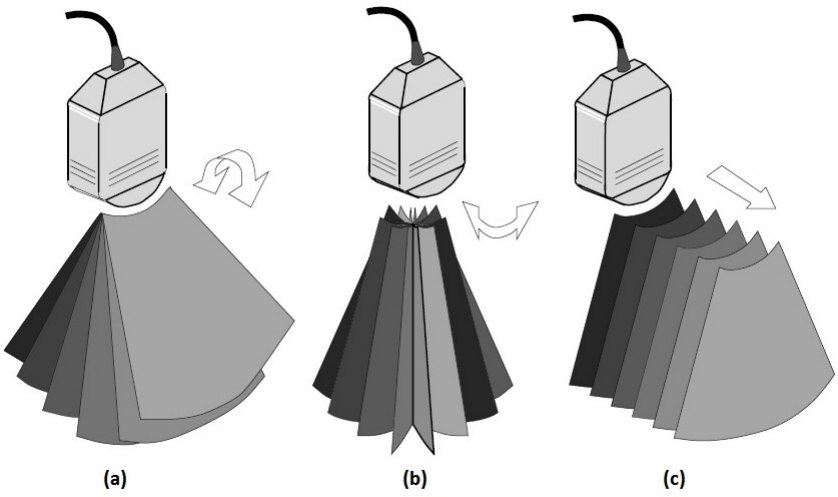

Figure 5: **Acquisition modes**: (a) Tilt scanning (b) Rotational scanning (c) Linear Scanning [27]

7.2.2 3D Free-Hand Imaging with Position Sensing

The approaches described above provide fast volume reconstruction times and high-quality 3D images. However the scanning apparatus is heavy and bulky that make the scanning difficult to perform in some cases [10]. Free-hand imaging allows the examiner to perform the scanning by moving the probe freely. In these methods images are not acquired in a predefined pattern, therefore, the examiner must ensure that there are no significant gaps between 2D images and that the spatial sampling is appropriate.

- ***Free-hand 3D imaging with magnetic field sensors***

In this method, a transmitter is used to create a spatially varying magnetic field and a position sensor which has three orthogonal coils that sense the magnetic field strength is placed on the probe. As the probe is moved, 2D images are acquired. Position sensor measures the position and orientation of the probe and images are stored with this information. Information from the position sensor is used to combine 2D images into a 3D volume of data. Position is measured relative to a transmitter which is fixed with respect to the patient's body [27]. Even though 3D imaging with magnetic field sensors overcomes bulkiness and weight problem that previously described approaches have, it has its own constraints. Electromagnetic interference from sources such as CRT monitors, AC power cables and electrical signals from the transducer itself can compromise the tracking accuracy. Additionally, if the magnetic field is sampled at a low rate or the probe is moved quickly errors in the calculation of the probe position will occur. As a result, there will be lag artifact in the image. However, this can be avoided by using a sampling rate around 100 Hz or higher [10].

- ***Free-hand 3D imaging with optical tracker***

An optical tracking system is used in this method to track the position and orientation of the probe by detecting a passive or active target (tool) that is attached to the probe. Tracking of the tool is done by using two (or more) calibrated cameras. A passive tool consists of three or more matt spheres at known relative positions on a small frame. An asymmetry in the arrangement of the spheres enables the tracker to calculate the orientation of the tool. An active tool may be formed from an arrangement of infrared light-emitting diodes (LEDs) that are excited in a known sequence. This can be done by the tracking software used with the cameras. As a result each LED can be identified and the orientation and position can be inferred [24].

Optical tracking systems are successful at locating absolute positions and orientations in 3D space relative to the calibrated cameras. Unlike position sensing from magnetic field, this system can provide an indication of whether each position reading meets a specified accuracy. This is because it is sometimes difficult to tell how much magnetic systems have been affected by metal in the environment. However, this method has the major drawback of requiring the clinician to maintain an uninterrupted line of sight between the cameras and the tracked objects attached to the probe [24, 10].

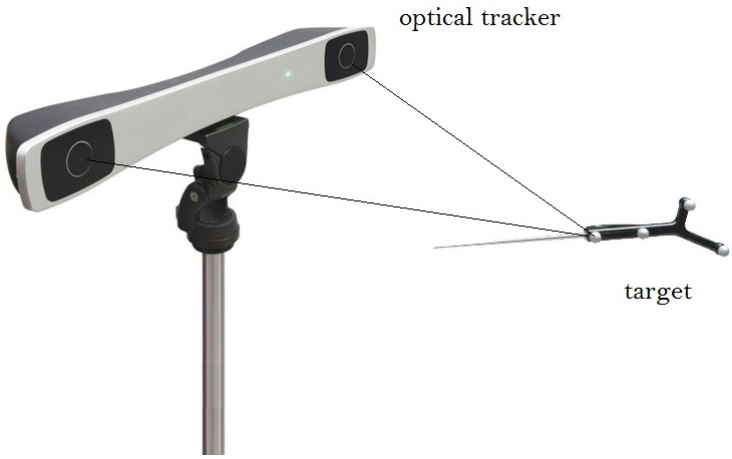

Figure 6: Imaging with optical tracker

- ***Articulated arm 3D scanning***

In this method, position and orientation determination is achieved by mounting an ultrasound probe on a multiple-jointed mechanical arm system. The position and orientation are calculated with the information provided by the potentiometers[4] that are placed at the joints of the movable arms. While moving the probe, computer stores the 2D images with relative angles of all arms of the system and with this information 3D volume is reconstructed. In order to avoid image distortions and errors arms must not flex. For optimal results arms should be kept as short as possible and number of joints should be reduced[10]. Therefore one must compensate between flexibility and 3D image quality.

- ***Acoustic 3D scanning***

In this method, three sound emitting devices are placed on the scanner probe and an array of fixed microphones are placed above the patient. The devices on the probe emit sound pulses while acquiring 2D images. Calculation of orientation and position of the probe is based on finding times-of flight[5] from each emitter to each fixed microphone. The microphones must be over the patient to have a direct line of sight to the emitters and the emitters must be close to the microphones to have a good signal-to-noise ratio [10].

Figure 7: Acoustic 3D scanning

[4]Resistance is related to the angle between the arms.
[5]Calculation is done with (1)

7.2.3 3D Imaging with 2D Probes

Unlike other methods described in this section, this approach uses a 2D array probe instead of a one dimensional (1D) array probe. In 2D array, elements are placed as a 2D matrix with similar number of columns and rows (e.g., 64x64). In this method the beam is electronically steered throughout the volume without moving the probe. Even though FOV is smaller than that is obtainable with mechanical swept volume method, the frame rate is higher. The maximum frame rate is around 20 volumes per second and to achieve this frame rate, the number of scan lines is limited and sampling volume is restricted in size [15]

Although this approach is being used successfully in echocardiology, problems like high cost of 2D transducer arrays, which results from requirement of electronic leads to be connected to the numerous small elements in the array, must be overcome [10].

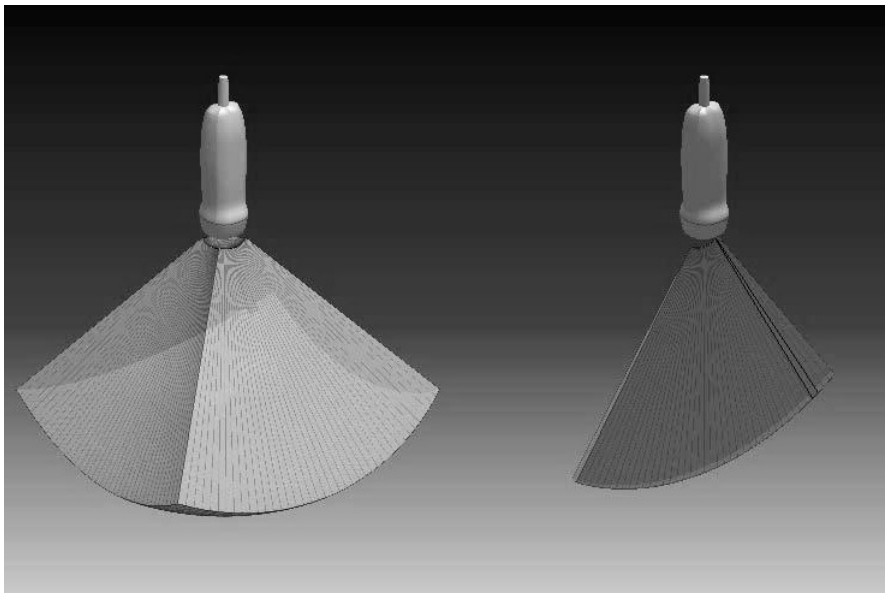

Figure 8: FOVs with 1D (right) and 2D (left) arrays

7.3 Summary and Comparison of 3D Ultrasound Imaging Methods

Considering the factors that have to be optimized for a 3D reconstruction without distortion, each method has its own advantages and disadvantages.

In mechanical swept volume methods, for sweeping the plane that is being imaged a motor is used and this makes the probe bulky and resolution is not the same for all parts in the volume of interest.

The articulated arm scanning method is inconvenient due to the fact that arms are not flexible. To increase the 3D image quality, the maximum size of the scanned volume and flexibility must be reduced.

The acoustic 3D scanning method is limited by requirement of line of sight during the process. In addition the velocity of sound varies with humidity and that causes distortions in the reconstructed volume [10].

In 3D imaging with magnetic sensors method, distortions arise from the magnetic field distortion while using 2D arrays for 3D imaging is costly and there are some problems before its use can become widespread in radiology [10].

The method with optical tracking system also needs a clear line of sight as in acoustic 3D scanning. But this problem can be handled by using more than one optical tracker.

Considering all methods that have been described, advantages of freehand systems are that they are cheap, require only existing, conventional ultrasound systems and relatively inexpensive additional components. Research into freehand systems is very active and several commercial systems have become available [25].

7.4 Requirements for Free-hand 3D Reconstruction

In free-hand imaging, instead of taking a instantaneous 3D snapshot, a 3D volume is created from a number of 2D scans. The motion of the probe is controlled by a physician and there is no restriction for movement of the probe. Therefore, the acquired B-Mode images can be at any position and orientation. This means pixels that make up 2D image lie at irregular locations in 3D volume and reconstruction of the volume can be regarded as unstructured, or scattered, data interpolation [26].

To be able to reconstruct a 3D volume without distortion, images and the probe positions at the time images are acquired must be synchronized accurately. One way to match positions and images is using time-stamps. Each image and

position information has a time-stamp and after grabbing the images and taking the positions these can be synchronized by looking at their time-stamps.

In addition to synchronization of images and positions, electrocardiographic recordings must be synchronized with these to choose the right image to reconstruct 3D volume. ECG is used for compensating for physiological motion, such as the cardiac pressure cycles in blood vessels. This is essential to ensure that such motion does not disrupt the integrity of the structure to be reconstructed [4]. Since pulsatile arteries will be imaged in this project, ECG data will be utilized.

Another part that has to be considered is temporal calibration of the position tracking device and ultrasound machine. One has to make sure that there are no latencies between time-stamps and images. It is possible that the image is time-stamped some time after it is actually acquired by the ultrasound probe. Temporal calibration involves calculating the difference between the image and position latencies. After calculation, the difference is added to the position sensor time stamps to synchronize the images and position [4] Similarly, latencies between position information time-stamp and actual time that the position information is taken must be considered.

Another calibration process is spatial calibration. The tracking system gives the position of the rigid body tool that is mounted on the probe. The position information is given with respect to a fixed reference, usually the transmitter. One has to make sure that the position of each B-scan pixel is accurate with respect to transmitter.

7.5 Electrocardiogram (ECG)

As explained in Section 7.4, ECG data is an important information in free-hand 3D imaging. The shape and size of an organ may change during the cardiac cycle. ECG data is used for deciding which image in a cardiac cycle will be used for reconstruction so that the size and shape of the organ is the same in all used images. Therefore it is worthwhile to explain basics of ECG.

An electrocardiogram is a recording of waveforms that are generated by the electrical activity of the heart. The signals are detected through metal electrodes attached to the chest wall and extremities of the body. Detected signals are then amplified and recorded by an electrocardiograph [20, 14].

ECG is a noninvasive, inexpensive and versatile test that is generally used for detecting arrhythmia, conduction disturbances and myocardial ischemia [20].

Contraction of any muscle is associated with electrical changes called depolarization, and these changes can be detected by attaching electrodes to the surface of the body [14].

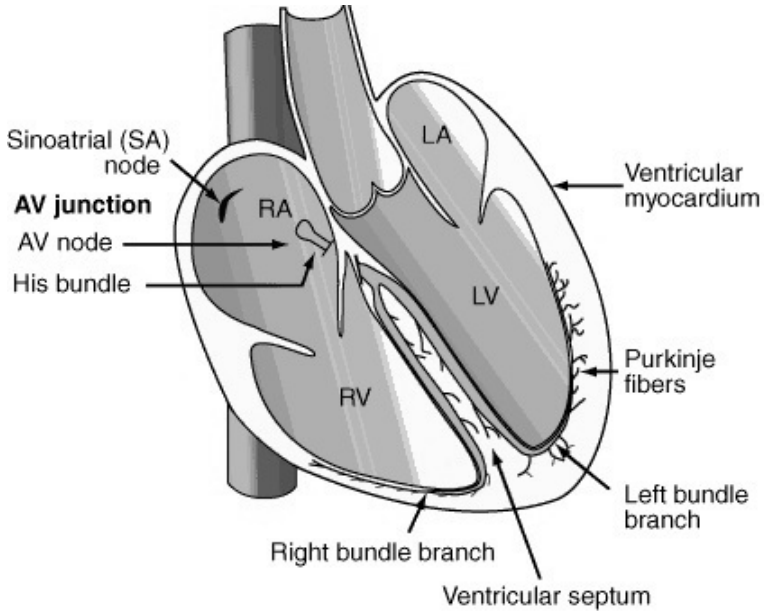

Figure 9: Schematic of the cardiac conduction system [20]

The depolarization stimulus for cardiac cycle normally starts in a special area of the right atrium (RA) called *sinoatrial* (SA) node (figure 9). Thereafter, depolarization is spread through the atrial muscle fibers. The depolarization spreads through *artioventricular node* (AV node) with a delay. After that, the electrical discharge travels rapidly to *bundle of His*, which divides the septum between ventricles into right and left bundle branches which rapidly transmit depolarization wavefronts to the right and left ventricular (RV and LV) myocardium by way of *Purkinje fibers*. The depolarization wavefronts then spread through the ventricular wall, triggering ventricular contraction [20, 14]

Result of these activities is seen as ECG waveforms (Figure 10) This waveform is used for synchronization in free-hand 3D imaging. A point in this waveform, for example R, can be used as a reference to choose the 2D image for reconstruction. In other words, all used images correspond to the point R in the cardiac cycle.

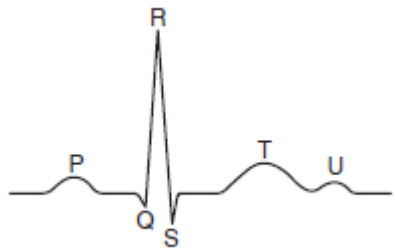

Figure 10: Basic ECG waveform

ECG *leads* are tracings of the potential difference between two electrodes and actually these are what recorded by the electrocardiograph. Since the electrodes are placed on different parts of the body, each lead gives a different view of the electrical activity of the heart and so a different ECG pattern. In this project 3 Lead Wire ECG System is used for recording ECG data.

7.5.1 The 3 Lead Wire ECG System

In this system three colored wires are connected to three electrodes to form a triangle (Figure 11). The three electrodes are colored yellow, red and green although these colors are not universal.

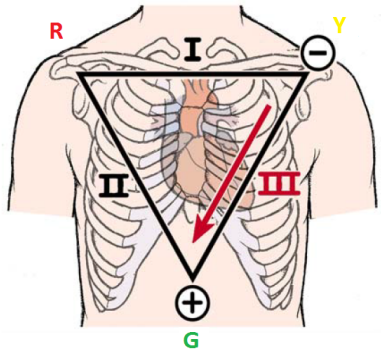

Figure 11: 3 lead ECG System

In an ECG test with 3 lead system, the red electrode is placed just below the clavicle (collarbone) on the right shoulder. This electrode has negative polarity in leads I and II.

The green electrode has positive polarity in leads II and III and is connected below left pectoral muscle near the apex of the heart.

The yellow electrode is connected below the left clavicle near shoulder and has positive polarity in lead I and a negative polarity in lead III.

Three lead system give three views of the heart where the views are from the perspective of the positive electrode towards the negative electrode [3].

Part III
Implementation of the 3DRec Application

8 System Setup

An example system setup for free-hand 3D imaging with optical tracker is presented in Figure 12. B-mode images and ECG data are streamed from the ultrasound scanner to a computer for storage and 3D reconstruction. Optical tracking system is connected to the computer for position information streaming. A target (tool) is mounted on the probe to acquire position and orientation of the probe during scanning process.

Setup for 3DRec, which is the software application that is developed for this project, is the same as shown in Figure 12. Ultrasound scanner, GE Vivid E9, and the computer are connected to the network via a local area network (LAN) cable. The optical tracker is NDI Polairs Optical Tracking System and the application, in principle is cross-platform but only tested in Windows.

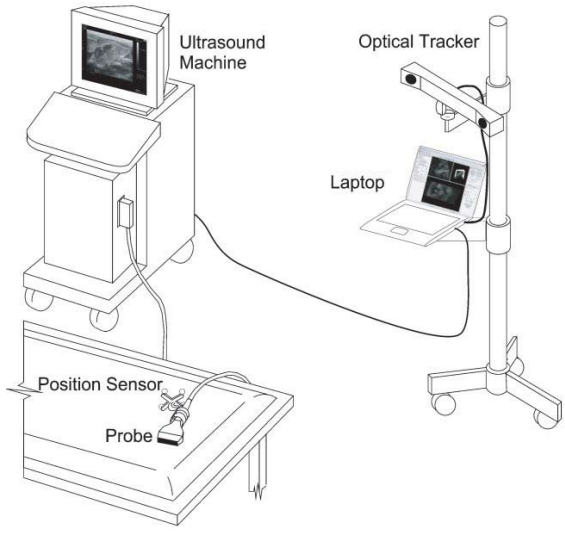

Figure 12: An example system setup for free-hand 3D imaging.

8.1 System Equipment

This section gives information about each utilized equipment used to realize a 3D reconstruction.

8.1.1 Polaris Spectra System

The Polaris Spectra System is an optical tracking system that measures the 3D position of active or passive markers attached to application-specific tools. The system has applications in industries such as medical, dental and research [17].

The Polaris Spectra System determines the position and orientation of the tools within a specific measurement volume. A 3D representation of the measurement volume is shown in Figure 13. The volumetric accuracy of the measurement in this volume is approximately 0.25 mm [17].

The position sensor is the main component of the system. The position sensor works as follows [17]:

1. The position sensor emits infrared (IR) light from its illuminators.
2. The IR light fills the surrounding area and is reflected back to the position sensor from sphere markers on passive tools. If an active wireless tool is used, the IR light triggers markers to emit IR light.
3. The position sensor measures the position of the markers and calculates the positions and orientations of the tools.
4. After calculation, the position sensor transmits the transformation data along with status information to the host computer for further processing.

The main components of the position sensor are:

- **Illuminators** Two arrays of infrared light-emitting diodes (IREDs) that emit the IR light for the detection.
- **Sensors** Two sensors that each employs a lens and a charge coupled device (CCD) for detecting the reflected light from passive tools or the emitted light from the active tools.
- **Indicator LEDs** The power, status and error LEDs

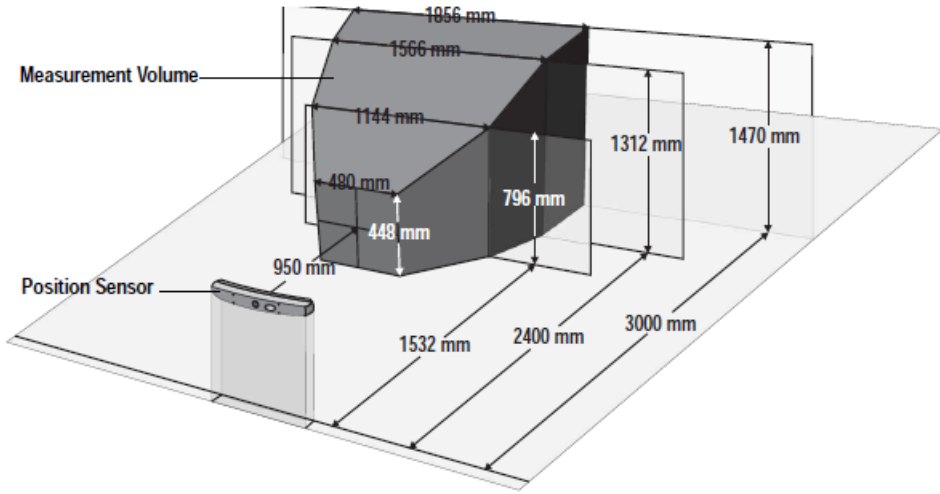

Figure 13: Polaris Spectra Measurement volume [17]

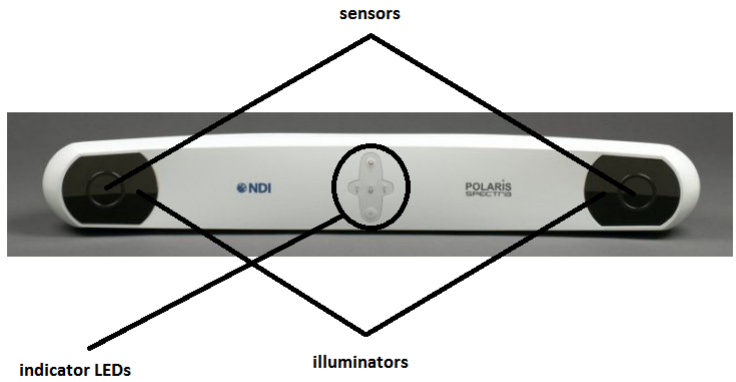

Figure 14: Position sensor front panel

Tools are rigid structures on which three or more markers are placed so that there is no relative movement between them. The tool that is used as a reference tool for evaluation of the program is shown in figure 15.

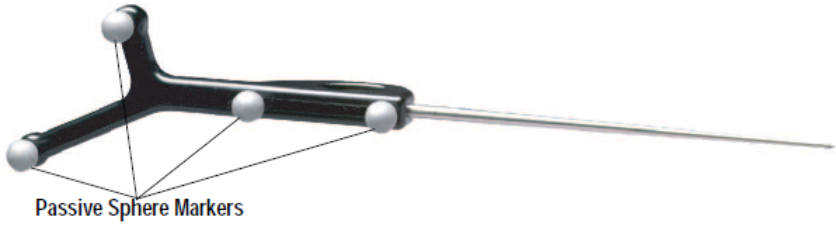

Figure 15: Passive tool [17]

It is a passive tool that has four passive sphere markers fixed on. These passive sphere markers have a retro-reflective coating that instead of scattering the IR light, reflects it back to its source. So in this system the IR light from the illuminators is reflected back from the markers directly to the sensors. The Polaris Spectra system can track the position and orientation of tools as well as the position of individual passive spheres [17].

8.1.2 GE Vivid E9 Ultrasound Scanner

The Vivid E9 ultrasound scanner is a high performance digital ultrasound imaging system. It provides image generation in 4D, 2D (B-Mode), Color Doppler, Power Doppler, M-Mode, Color M-Mode, PW and CW Doppler spectra, Tissue Velocity imaging, Advanced Strain and Contrast applications. An overview of the major system components of Vivid E9 is given in figure 16.

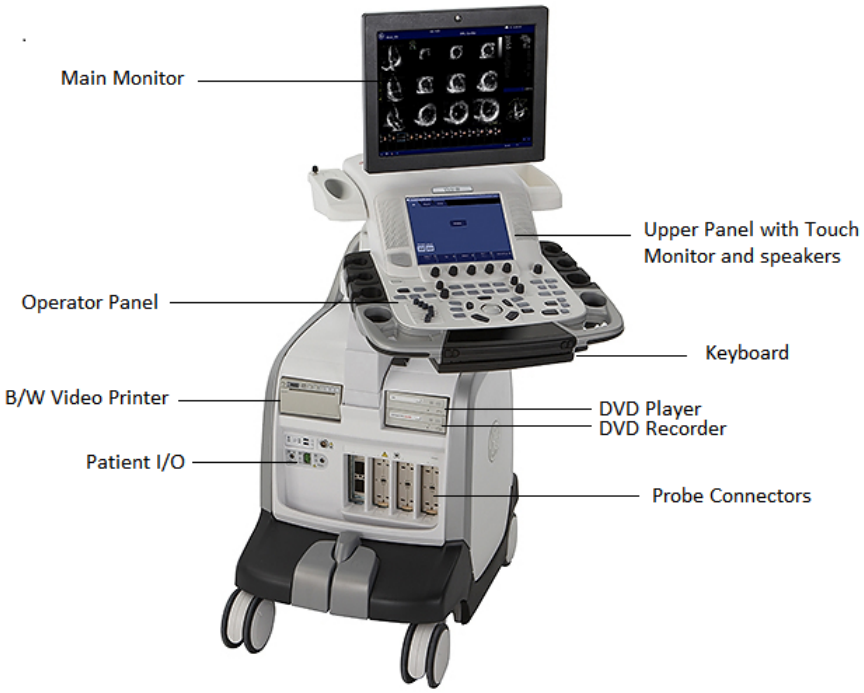

Figure 16: Vivid E9 major components

8.1.3 GE 11L Linear Probe

This probe is used in applications like vascular, breast, small parts and thyroid. It is a linear array[6] probe with 4.5-12.0 MHz bandwidth. FOV of this probe is 39 mm.

The probe is connected to probe connectors in the front panel of the ultrasound scanner.

Figure 17: GE 11L linear probe

8.1.4 ECG on Vivid E9

Instead of using a separate ECG device, ECG module on Vivid E9 ultrasound is used in this project for acquisition of ECG data.

As explained in Section 7.5.1 3 lead ECG is used for acquisition of ECG data. Three electrodes with colored wires are connected to the trunk cable. The trunk cable is a single cable that is connected to the ultrasound scanner at one end and provides a splitter device at the other hand. The trunk cable is plugged into the patient I/O port on the scanner.

[6] A multielement transducer in which elements are positioned one after another in a row. The image format is rectangular [15].

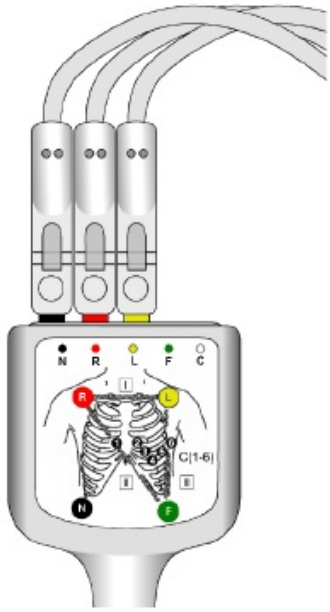

Figure 18: The trunk cable

9 Software Tools

This section provides brief descriptions of the software materials used for implementation of 3DRec application.

9.1 The Visualization Toolkit 5.10

The Visualization Toolkit (VTK) is a freely available C++ class library for 3D graphics and visualization. The toolkit enable complex applications to be built from small pieces [28]. 3DRec application is developed mainly using this library.

9.2 Qt 4.8

Qt is a comprehensive C++ framework for developing cross-platform application with a graphical user interface [6].

Qt Designer is the visual design tool of Qt for designing and building GUIs. It gives more options to programmers by providing a visual design capability. Qt framework is used to create the GUI for the application.

9.3 GEStreamer Library and DataStreamClient Application

GEStreamer library is developed by Gabriel Kiss, a researcher at the Department of Circulation and Medical Imaging at Norwegian University of Science and Technology (NTNU), and researchers from SINTEF research organization. This library is developed to stream and save B-mode image, color flow image and ECG data from GE Vivid E9 ultrasound scanner. DataStreamApplication is created to test the GEStreamer library code. It basically displays the streamed image and ECG data.

A structure overview of the application is given in Figure 20. Main part of the application is vtkEchoStream which is a source object that reads a stream from the ultrasound scanner. It consists of two parts: ThreadStream, which contains all the code for data streaming from the ultrasound scanner and vtkRawStreamData which holds a streamed image with optional additional information.

vtkEchoStream code includes a circular buffer for saving streamed information on memory. Size of this buffer is 100 elements for 3DRec application and this size can be increased or decreased if desired.

Each element of the buffer, which will be referred as a frame here after in the report, is a vtkRawStreamData class object. It mainly contains streamed image,

ECG data and corresponding ECG times to this data. For more information about circular buffer and content of the circular buffer of GEStreamer library see Appendix A.

ECG data is streamed separately as ECG values and ECG times. There is one second of values and times in one buffer element. ECG values are the amplitude of ECG signal while ECG times are the time-stamps of ECG values. Relation between the ECG times and ECG values is shown in Figure 19. Sampling rate of the scanner is approximately 600 samples/second, therefore 1200 samples correspond to nearly two seconds of data.

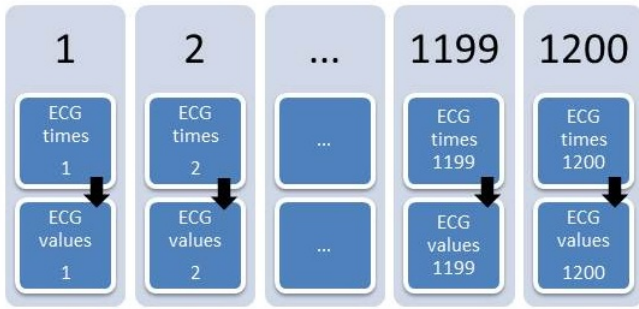

Figure 19: ECG times and values

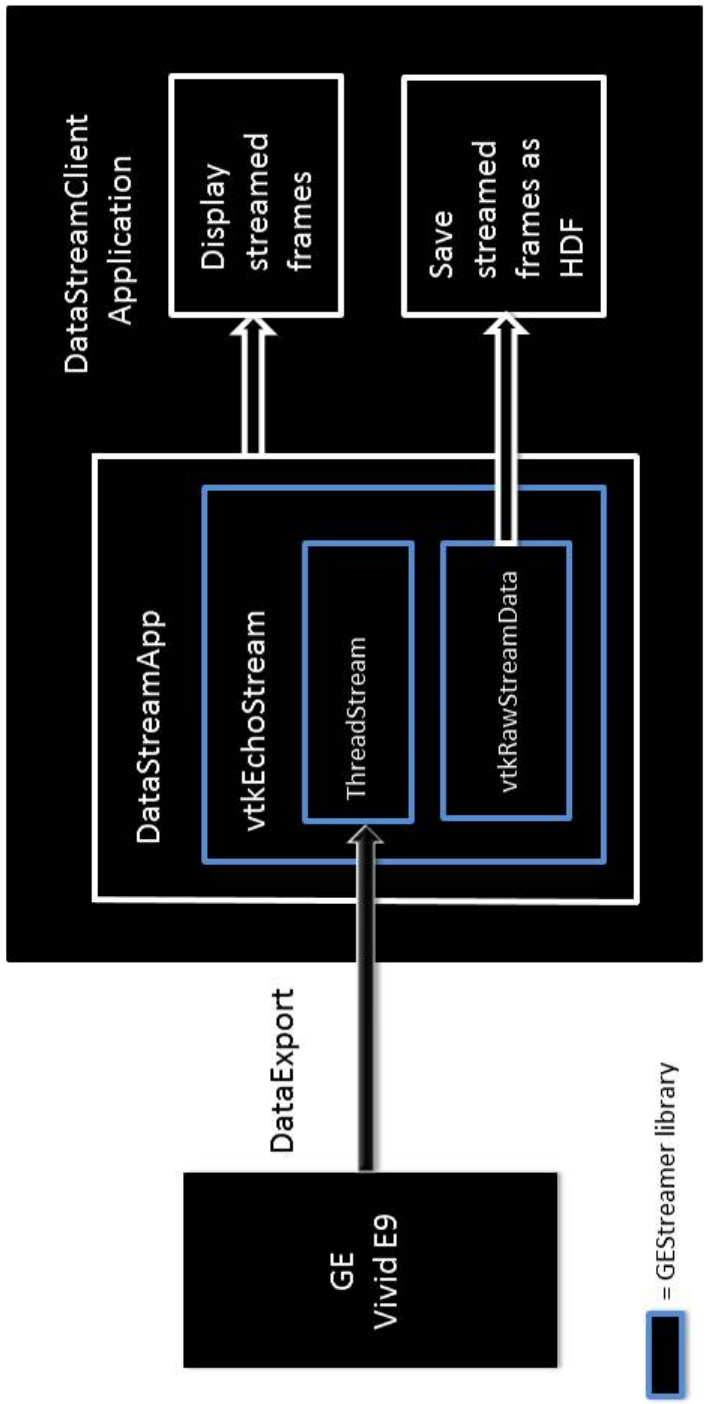

Figure 20: DataStreamClient application structure

ThreadStream is the thread where the data is streamed from the scanner. The whole process in this code is thread safe. In other words, it is assured that when data is being written into the circular buffer or a new streamed data is assigned to a variable, data cannot be accessed by another part of the code.

Streamed data can be saved as .hdf (Hierarchical Data Format) files if desired. HDF is a file format for storing large amounts of numerical data in a natural manner. It allows direct access to parts of the file. Therefore, it is easy for the user to interpret and access the saved data. As mentioned before vtkRawStreamData holds the streamed data from the scanner, therefore content of the vtkStreamData is written to an .hdf file for storage. In Figure 21 an example of the saved .hdf file content is shown.

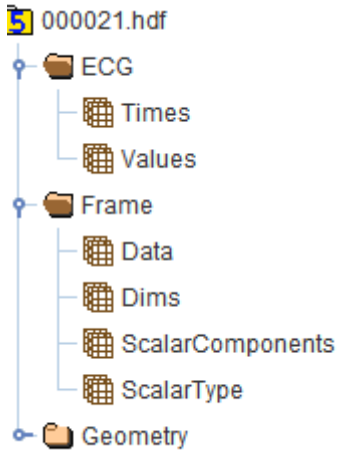

Figure 21: hdf content

10 Developing the 3DRec Application

This section presents the methods used for developing the 3DRec application. Firstly an overview of the application is given and then the implementation of the application is described in details.

3DRec application is developed in the C++ programming language. GEStreamer library is used for streaming between the ultrasound scanner and the computer (client). The library is modified in order to connect to the optical tracking system. Information sent from the tracker is also saved in vtkRawStreamData. Therefore it is included in each frame with the information streamed from the ultrasound scanner. An overview of the connection between streaming related classes is given in Figure 23.

As can be seen from Figure 23 streaming between the ultrasound scanner and the computer is one way. The stream is only from the scanner to the computer and the streamed data is mainly ultrasound image and ECG data.

Communication between the tacker and the computer is two-way. Commands, such as make a beep sound or start tracking, are sent from the application to the optical tracking system while position and orientation information is sent from the system to the computer.

Connection between the libraries and the application structure is shown in Figure 22.

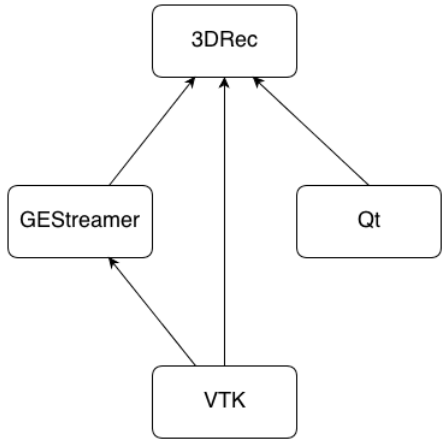

Figure 22: Structure of the 3DRec application

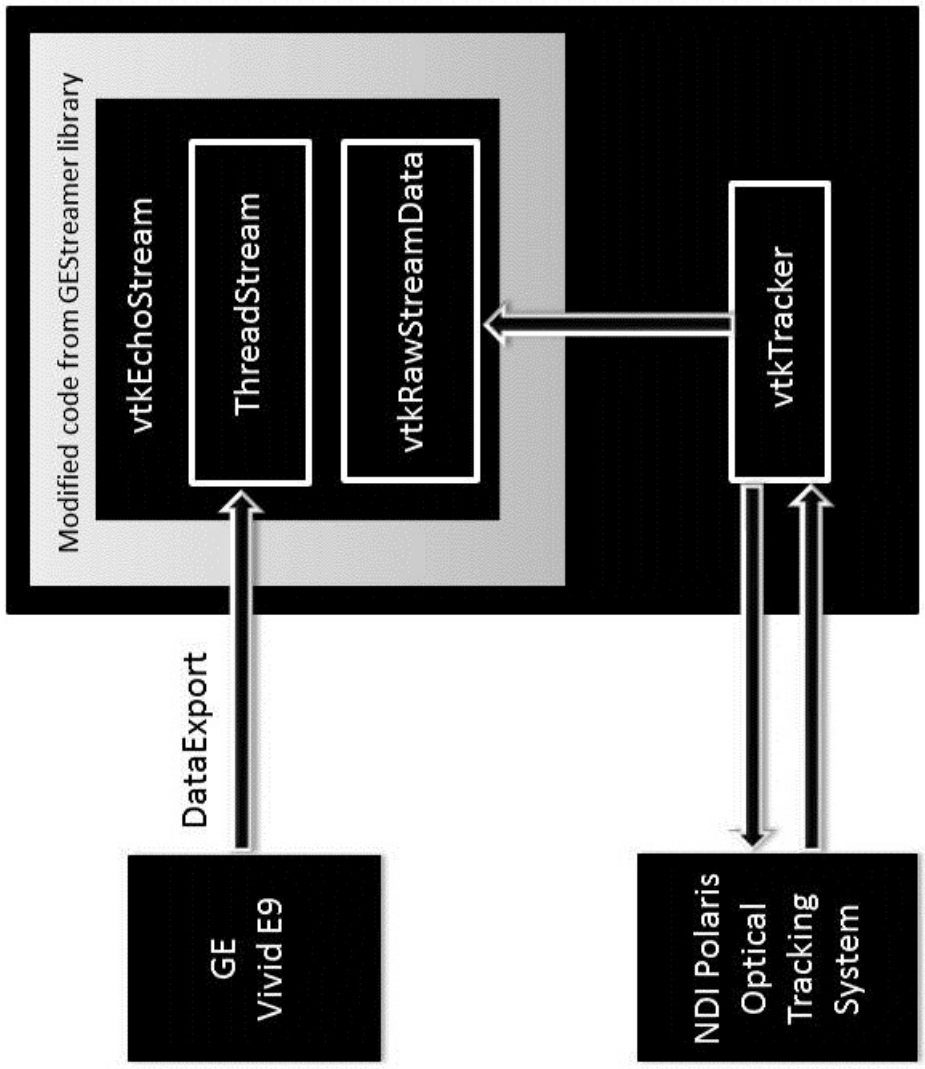

Figure 23: Data Stream Application structure and overview

The application is developed for 3D reconstruction of artery geometry and flow. Implementation details of the features of the application is given in the order of program flow.

As the application starts, it first attempts to connect to the ultrasound scanner. If the connection is successful then it attempts to connect to the tracking system. In case the connection to the scanner fails, the user is warned and the application stops. If the connection to the tracking system fails, the program runs without streaming information from the tracker.

10.1 Interaction with Optical Tracking System

10.1.1 Connection to the Optical Tracking System

Interface between the application and the tracking system is achieved by vtkTracker and vtkTrackerTool classes that are available as open source codes.

When the application starts, it checks if the tracking system is connected to the computer and notifies the user with a warning whether tracker is available.

In case the tracker is connected, the application looks for the .rom file that is specific to the tool that will be used. These files are called *tool definition files*. Information like geometry of the tool's markers and tool's manufacturing data are stored in the tool definition file [17]. If it is found, the tracking system is forced to start tracking and make a beep sound to notify the user that tracking has started by sending commands to the tracking system. If either the tracker is not connected or .rom file cannot be found, the application continues without trying to connect to the optical tracking system again and all further steps are done without position and orientation information.

10.1.2 Streaming from the Optical Tracking System

vtkTracker starts up as a separate thread after the connection is established between the tracker and the application. Information streamed from the system is saved to a tracker buffer provided by vtkTracker class. The size of this buffer is 1000 for 3DRec application.

ThreadStream code from the GEStreamer library is modified in order to stream from the tracking system. Image and ECG data are streamed and saved to the circular buffer in streaming thread. In addition to these data, now last computed 1000 position and orientation information is assigned in the same frame as the newly received image and ECG data.

Data received from the optical tracker are time stamped. The timestapms are the elapsed time in seconds from 1970 to the position and orientation calculation time. The timing precision of the tracker is sub-millisecond even though the values are stored in seconds

The content of one frame before and after modification is depicted in Appendix A.

10.1.3 Information streamed from the tracking system that is used by the application

Even though the packets received from the tracker contain more information, information that is used by the application is as follows:

- the position of the tool's origin in the coordinate system of the position sensor

- orientation of each tool

- information about status of the tool indicating if the tool is out of volume, partially out of volume or missing.

vtkTrackerTool class provides the first two information as a transformation matrix. For more information about transformations see Appendix D.

10.2 Display the Streamed Data

10.2.1 Live View Window

Live View window is created with a QVTKWidget to display the streamed ultrasound images and last three seconds of ECG data. The role of this widget[7] is to provide a way to display VTK data (image and ECG data in this case).

Stream rate from the scanner is approximately 30 images per second and the window is updated with a new image every 10ms. This causes a delay between the live image and the image displayed on the computer. Therefore instead of rendering all received images, the last received image is rendered every 10 ms in the Live View window.

This window is placed next to the 3D View window so that the user is able to see the position of the image plane in 3D and the live image together. This enables the user to choose the most informative and appropriate imaging plane for 3D reconstruction.

[7] "a widget is a visual element in a user interface" [6]

10.2.2 3D View Window

3D View window is created with a QVTKWidget like Live View window. A probe model and a rectangle object created with vtkPlaneSource are rendered in this window.

Position and orientation of the probe model and the plane in 3D coordinates are calculated by the received information from the tracker. Probe object imitates the movement of the real probe. This enables the user to see probe position relative to the previously registered slices. The reason that a plane object is attached to the probe is to show the user the position of the slide that will be captured.

Sections 10.3 - 10.6 explain the process that starts after *Capture* button is clicked. Once the button is clicked, it is deactivated until the process is over. Therefore this process cannot be aborted by the user. The aim of this process is to acquire images from a chosen position for one cardiac cycle and add an image into the 3D View window for reconstruction.

10.3 Capture the Streamed Data

Data capturing starts when the user clicks the *Capture* button. This push button is created with a QPushButton widget in Qt Designer.

Capture button starts the data capture process if an ECG update is performed previously. Otherwise, first click calls an ECG update.

The first action that is taken in the data capture process is to start a timer and continue streaming images from the chosen position. The timer interval is set to twice of the median interval length found by the ECG update algorithm. This assures that there will be at least one cardiac cycle in the acquired ECG data and that the user does not have to wait more than needed. A progress bar is provided to inform the user about the acquisition progress.

An important criteria for an acceptable reconstruction is to keep the probe still once the most informative position is achieved. To notify the user whether the probe is kept in the same position during the acquisition time, the color of the progress bar is set to green or red indicating that the probe has not moved (Figure 24a) or moved (Figure 24b) respectively.

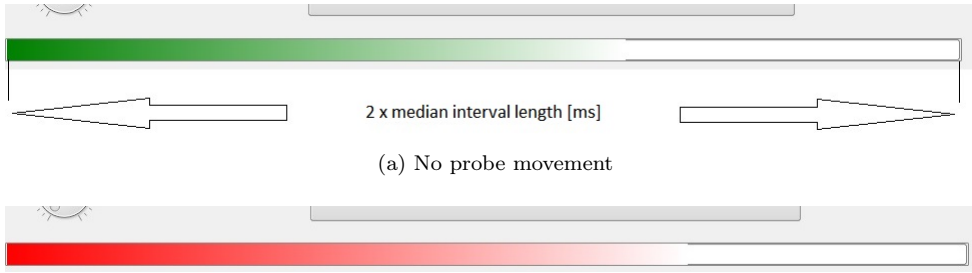

(a) No probe movement

(b) Probe is moved

Figure 24: Progress bar of the data capture process

Keeping the probe in the same exact position throughout the acquisition interval is difficult for the user. In addition, even if the probe is kept completely still there may be small changes in the position due to the fact that the optical tracking system has an error probability. Therefore a reasonable[8] tolerance is introduced in the calculation. The user is warned with the red color in the progress bar if position of point P in Figure 25 at the time capture button is clicked differs 2 mm from its position at any time during the acquisition interval.

[8]The criteria for reasonableness is intuitive and based on the idea that the image will be rotated about the origin of the transducer and a point away from the origin will be more sensitive to rotation.

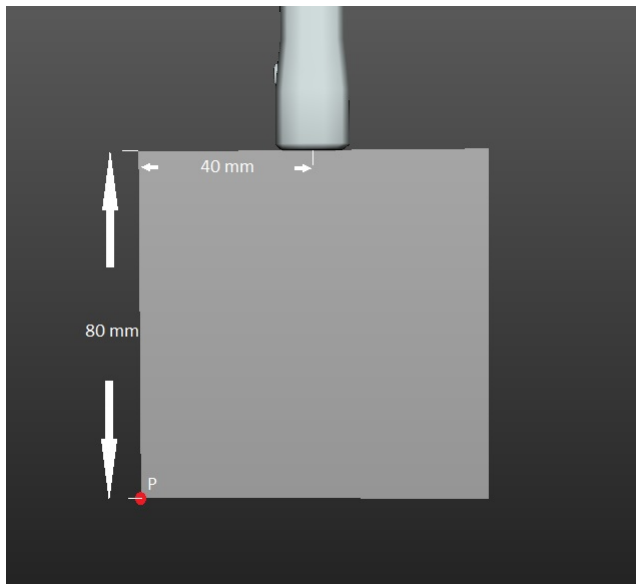

Figure 25: Error calculation point

When the elapsed time starting from the moment capture button is clicked is equal to the timer interval, streaming from the scanner is stopped and no new information is written to the circular buffer.

10.4 Find ECG Signal Parameters and Peak Points

Data capture process is followed by extracting three seconds of ECG data from the ECG buffer. This ECG data is then used for peak detection.

10.4.1 ECG Update

As stated earlier, before starting capturing data ECG update has to be performed. ECG update is the process of computing the main parameters of ECG signal for peak detection. These are basically a threshold and the median interval length of the ECG signal. Parameters are shown in Figure 26. Since these parameters are calculated from the ECG signal, values of these parameters vary with the signal. Therefore the peak detection is an adaptive process.

The algorithm used for ECG update and peak detection (Section 10.4.2) is a slightly modified reimplementation of an algorithm developed by Sigurd Storve, who is a PhD candidate in medical imaging at NTNU.

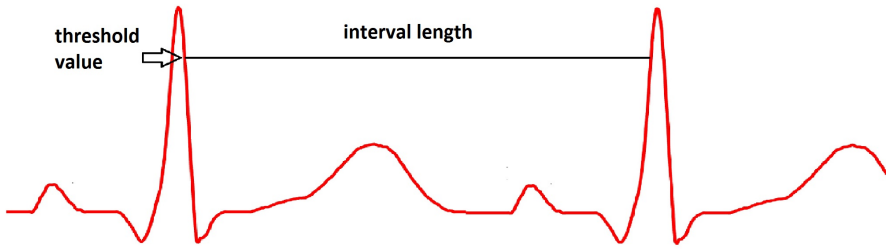

Figure 26: Calculated ECG parameters

ECG update must be called before finding peaks in the signal. At least three seconds of ECG data must be streamed from the scanner to perform the ECG update. This is called adaptation time. Three seconds of data usually contain at least two complete cardiac cycles. As more than one different interval length will be found in the signal, the median of the interval lengths is used for peak detection. The algorithm for ECG update can be found in Appendix B.

10.4.2 Peak Detection

Peak detection can be defined as finding the peak points (point R in Figure 10) in an ECG signal. Once the ECG parameters are calculated, finding peaks in ECG signal is straight forward. The algorithm can be explained in five steps:

1. Find the first point above threshold value (point 1 in Figure 27)
2. Save ECG values for 0.3 x median_interval_length (values between points 1 and 2)
3. Find the maximum value in saved values. This value is a peak point. Return the time stamp corresponding to peak value.
4. Skip the values between point 2 and 3 since we are sure that there will not be another peak between these points.
5. Go to step 1.

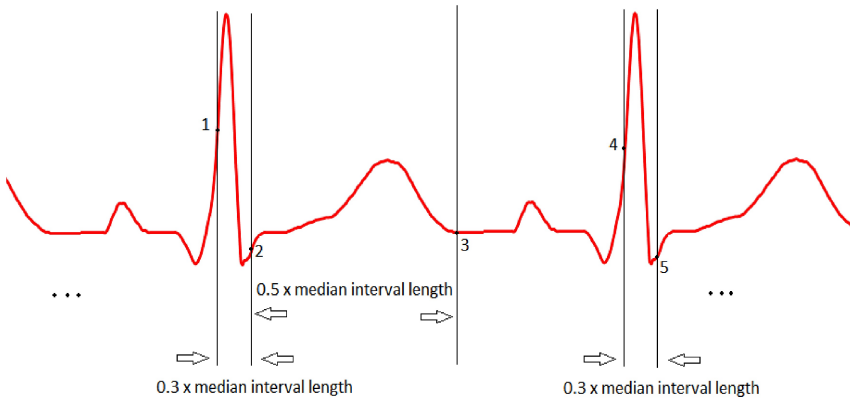

Figure 27: Peak detection algorithm

Timestamps of the found peak values are written into a vector. In case no peak value is found, the user is warned with "*No peaks found! Try again for the same position!*" message, the data capture process is terminated and streaming starts again.

10.5 Synchronization of the Captured Data

Synchronization of the captured data is the most important step as it determines the quality of the reconstruction. This step determines not only the image that will be registered in 3D coordinates but also the position and orientation of this image.

- ***Get timestamps of the images***

After peak detection timestamps of the images in the circular buffer are written into a vector. Images and ECG data are timestamped on the scanner side. Therefore they are timestamped using the same time axis.

- ***Find "peak images"***

Stream rate of the scanner is approximately 30 images and 600 ECG values per second. Image and ECG acquisition is done asynchronously. As image times are important for the reconstruction rather than the peak times of the ECG signal, in this step the images whose time stamp is closest to the peak times are found and position of these images (peak images) in the circular buffer is saved to a vector.

- ***Extract heart cycles***

One heart cycle duration is regarded as the time interval between two peak points in the ECG signal. Positions of the peak images are found in the previous step. In this step, all images between the found positions are saved to a vector. In case there is more than one heart cycle in the ECG signal, the cycle whose starting time is closer to the peak time is chosen. For example, assume that the found peak image positions are [20,50,80] (The size of the circular buffer is 100). This means there are two heart cycles in the ECG signal; one between 20 and 49 and the other between 50 and 79. If the image at position 20 is closer to a peak time than image at position 50, images between 20 and 49 are saved to a vector. Otherwise images between 50 and 79 are saved.

In case only one peak value is found in the ECG signal, the user is warned with "*Could not extract any cycles! Try again for the same position!*" message, the process is terminated and streaming starts again.

- ***Find the tracking matrices and save synchronized data***

Received images are also timestamped on the client side with IGSTK[9] real-time clock. This clock returns the time as elapsed time from 1/1/1970 in milliseconds. This timestamp is comparable with the timestamp of position and orientation information received from the optical tracker. The difference is that the tracker time stamp is in seconds.

The problem with using timestamps created on the client side (by the application) is the delay between the image formation on the scanner side and receiving the image on the client side. Temporal calibration is needed to overcome this problem. The method used for temporal calibration is explained in Section 10.5.1. The outcome of the temporal calibration is the delay in ms. This delay is subtracted from the client side time stamp and the tracking information corresponding to the time stamp is found in the tracking buffer that is provided by the vtkTracker class.

After the image and tracking matrix are synchronized, they are saved into a vector. Each element of this vector contains

- B-mode images belong to the chosen cardiac cycle
- Tracking matrices corresponding to the images
- ECG data starting from two seconds before the peak image time stamp and ending three seconds after the peak image time stamp.

10.5.1 Temporal Calibration

Temporal calibration is done with CustusX[10] software. This software also uses GEStreamer library to stream images from GE Vivid E9 ultrasound scanner and NDI Polaris tracking system is used for the calibration. Therefore temporal calibration delay calculated by this software can also be used for the developed 3DRec application.

The setup for the computation of temporal delay is shown in Figure 28.

The bottom of a plastic container is imaged in this experiment. The container is filled with water and the probe is moved up and down as shown in Figure 29a for approximately three seconds for the delay calculation. An acquired image is shown in Figure 30. Line A in the figure corresponds to a vertical line drawn from the middle point of the transducer. The procedure explained below is followed to compute the delay

[9] The Image-Guided Surgery Toolkit (IGSTK) is a framework used for image-guided surgery applications.

[10] Information about the software and how the temporal calibration is done can be found in [2].

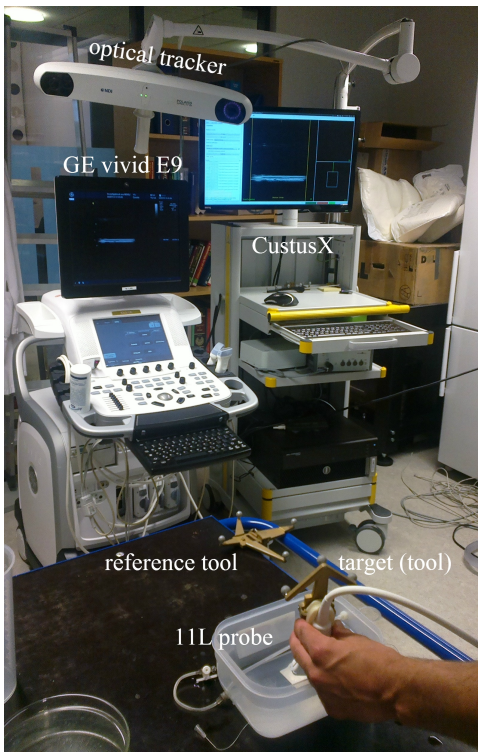

Figure 28: Temporal calibration setup

- Find the first point in the image that has a non-zero value and intersects with the line A
- Calculate the movement of the point from acquired images
- Calculate the probe movement from the tracking information.
- Compute the time shift from the movements calculated in steps 2 and 3. A possible movement is shown in Figure 29.

Streamed images are timestamped when received on the client side therefore the delay is subtracted from the tracker timestamp to for synchronization.

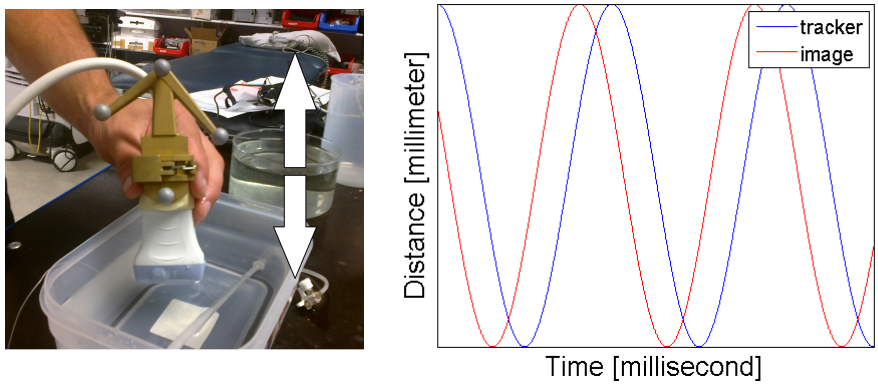

(a) Probe movement

(b) Possible resulting movements found from collected images and tracking information

Figure 29: Temporal calibration

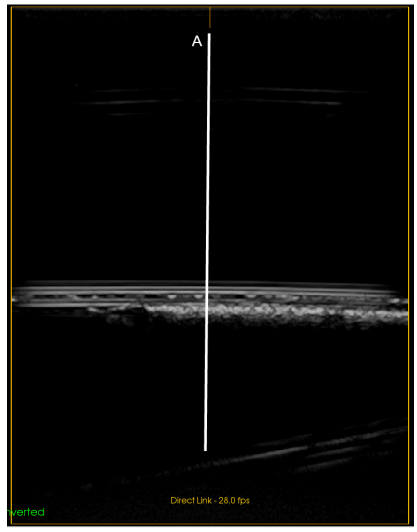

Figure 30: A sample image used for temporal calibration

10.6 Registration of Synchronized Images

As carotid is a pulsatile artery, its diameter changes during one cardiac cycle. Therefore, images that will be used for 3D reconstruction must be synchronized in time. More accurately, images must correspond to the same phase of the cardiac cycle.

One B-mode image is registered in the 3D View window each time the capture button is clicked. This registered image is the peak image of the previously chosen cardiac cycle. All images are synchronized with the tracking in formation in the previous step. Using this information ultrasound image is added to the 3D scene in the correct position and orientation. This process requires a spatial calibration and a couple of coordinate system transformations.

As shown in Figure 31, B-mode image, tracking tool, position sensor and VTK have their own coordinate systems. The transformations between the coordinate systems will be represented by the letter "T". A transformation from coordinate system A to coordinate system B will be represented as $T_{B \leftarrow A}$. More information about 3D coordinate system transformations can be found in Appendix D.

Probe calibration is necessary to find the transformation from the coordinate system of the B-mode image to that of the tracking tool. Transformation matrix that transfers a point in B-mode image coordinates to the tool's coordinate system is provided by SINTEF. This transformation is represented as $T_{M \leftarrow I}$ where "I" represents image coordinates while "M" represents the tool's coordinate system. Instead of the letter "T", "M" is used to avoid confusion.

The tracking system returns the position and orientation information of the tool's origin in the position sensor's coordinate system (global coordinate system) and this information is given as a transformation matrix by vtkTracker class. This transformation is represented as $T_{G \leftarrow M}$. In addition, if desired another tool can be set as a reference tool by using vtkTracker class. If a tool is set as a reference tool, it's coordinate system becomes the global coordinate system in which other tools are tracked [17].

To visualize the image in coordinate system of VTK, a transformation matrix is created. This transformation transfers a point in global coordinate system to VTK coordinate system. It is represented by $T_{V \leftarrow G}$.

To visualize a point p_p in 2D image as a voxel (p_V) in VTK coordinate system, pixel coordinates are multiplied with the transformation matrices in the following order

$$p_V = T_{V \leftarrow G} T_{G \leftarrow M} T_{M \leftarrow I} p_p$$

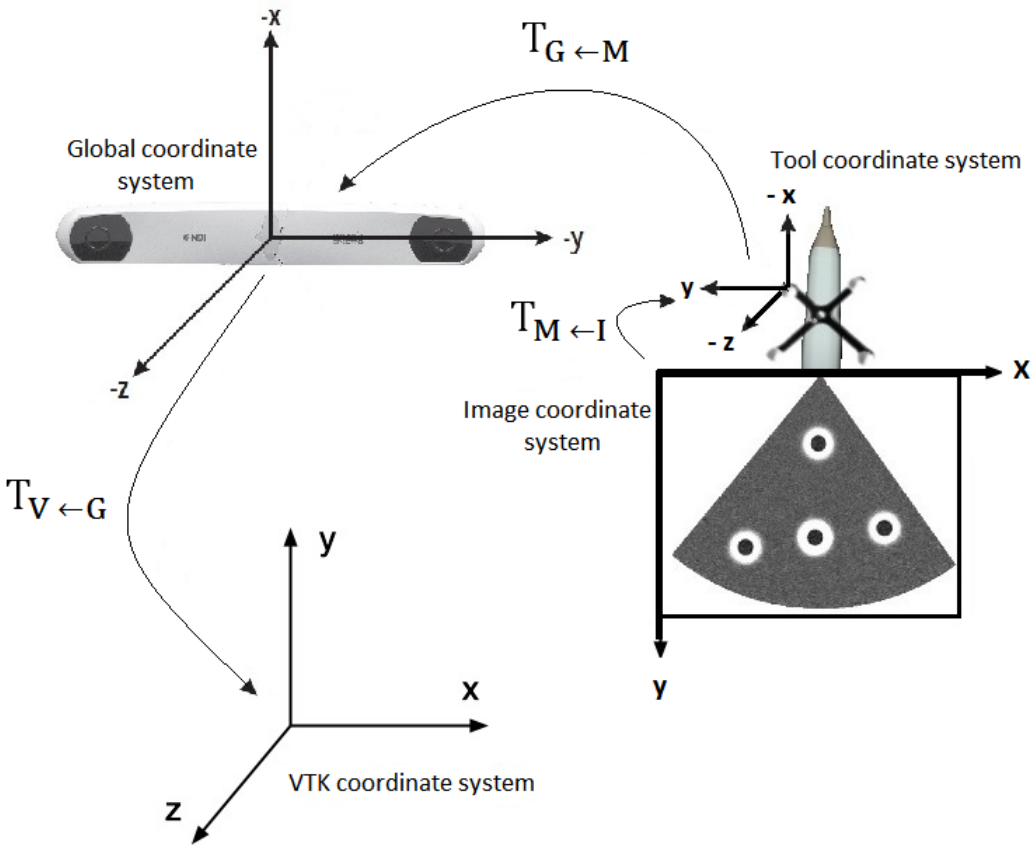

Figure 31: Coordinate system transformations needed to transform a point from image coordinate system to VTK coordinate system

10.7 Additional Features

This section presents the useful additional features of the 3DRec application.

10.7.1 Manual or Automatic ECG Update

In case the ECG signal changes during the 3D reconstruction, the peak detection algorithm will fail to find the peak values in the ECG signal. To overcome this problem an "ECG update" button is provided. This button runs the ECG update algorithm explained in Section 10.4.1.

It is also possible to update ECG parameters automatically each minute. If "Update ECG automatically" check box is checked ECG parameters are updated every 60 seconds.

10.7.2 ECG Gain

ECG signal amplitude changes from patient to patient, lead to lead [33] as well as for different in vitro testing environments. This causes the image being displayed in Live View window to shrink when the amplitude is high. If the amplitude is low, then the ECG signal is almost a straight line in the Live View window.

An ECG gain dial button is provided in the GUI to adjust the amplitude of the ECG signal. This ensures a proportional view of ECG signal and the B-mode image.

10.7.3 Segmentation

It is sometimes possible that visualization of only Doppler (flow) data is more informative than color flow image. Specifically, if the geometry of the artery is needed to be displayed in 3D.

The "Show only flow" check box is used for this feature. If the check-box is checked, a created segmentation algorithm is applied on the slice that will be added to the 3D scene.

This segmentation is done basically by setting the opacity of the image pixels that do not have flow information to zero.

10.7.4 Analyze Captured Data

Data that is stored on the memory can be analyzed using analysis module of the application. The analysis window enables the user to replay the captured

cardiac cycle images synchronously. User can choose how many cycles will be replayed at one time by using "number of windows" drop down list. Options are: 2, 4 and 6 cardiac cycles.

It is also possible to incorporate tracking information for analysis. This gives the opportunity to the user to see how probe was moved during the acquisition of the images. The user can choose this option by using "show movement" check-box.

10.7.5 Save Data

Captured data is stored on the memory but it is not possible access this data once the application is closed. Data on the memory can be saved to the hard disk to be analyzed further with different programs or to be transferred to other computers.

Captured data is saved in .hdf file format. HDF related parts of the GEStreamer library is modified to use in 3DRec application. The structure of the file is shown in Figure 21.

- The file name is set as the date and time that file is created. Format is: day.month.year_hour.minute.hdf
- The slice group contains captured images from one position for one complete cardiac cycle time, five seconds of ECG data and number of slices. Slices are enumerated starting from zero and number of slices correspond to number of saved cardiac cycles.
- The frame group mainly contains B-mode image in raw and scan converted forms, time stamp of the image, tracking matrix corresponding to the image time, a flag, IsTrackingValid, indicating whether the probe was in the measurement volume of the tracking system or not.

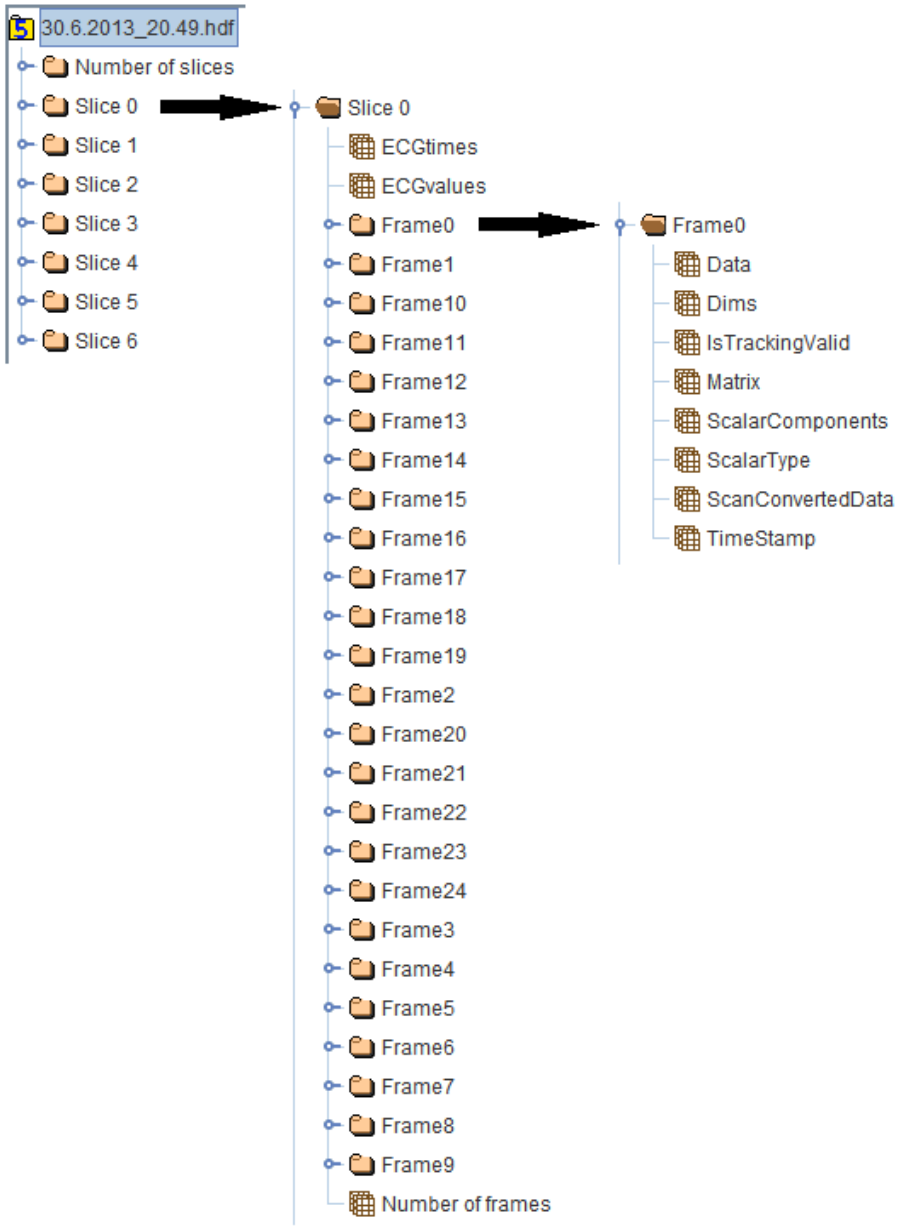

Figure 32: hdf file structure for 3DRec application

10.7.6 Delete Last Slice and Delete All Slices

Two push buttons are provided to remove slices from the 3D reconstruction. Button "Delete last" removes the last added slice from the 3D scene and deletes the last captured cardiac cycle images and matrices and ECG data corresponding to that images.

"Delete all" button deletes all saved data on the memory so that the reconstruction can start from the beginning.

10.7.7 Use A Reference Tool

A reference tool can be used to show the position of the probe in a coordinate system other than position sensor's.

A reference tool is useful if the object being imaged is not stable. If the reference tool is attached to the object, the probe will be in the same position in the coordinate system of reference tool even if the object is moved.

This option is provided with "use reference tool" check-box.

Part IV
Validation Setup and Experiments

Another point that is as important as developing the application is its validation. This part presents the tests performed for validation of the 3DRec application. Firstly, specifications of the equipment used for the experiments are given briefly. This is followed by explanation of the methods applied for validation.

11 Evaluation Tools

This part describes the equipment used for validation purposes.

11.1 Signal Generator

Agilent 33522A Function Generator is used for simulating the ECG signal. It is possible to generate arbitrary signals with the generator. Pure and distorted ECG signals are created with MATLAB and saved as .csv files. These files are then imported to the function generator via its USB port. Output of the generator is connected to the ECG leads of the ultrasound scanner.

Figure 33: Agilent 33522A Function Generator

11.2 Flow Generator

Blood flow is simulated by a Shelley Medical Imaging Technologies, PhysioPulse flow system. The generator is connected to a computer via USB port and the user can choose a waveform and modify its parameters, such as amplitude (pressure) and frequency. Sine shaped and flat waveforms are used for simulating pulsatile and constant flow respectively.

Figure 34: Shelley Medical Imaging Technologies, PhysioPulse flow system

11.3 Flow Phantom

Flow phantom is used for simulating a vessel for spatial positioning evaluation of the application. The phantom contains four flow channels which have 2,4,6 and 8 mm diameters. Flow channels are located 15 mm below the scan surface. Dimensions of the phantom is given in Figure 35.

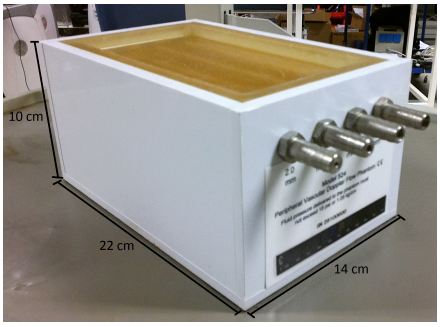

Figure 35: Flow phantom dimensions

12 Validation Experiments

The aims of the validation experiments are to

- demonstrate how well peak detection is performed with clean and distorted ECG signals,
- demonstrate how well cardiac cycle extraction is performed with clean and distorted ECG signals,
- calculate how accurately a slice is positioned in the 3D scene,
- demonstrate how using a reference tool affect the spatial positioning accuracy,
- show how artery diameter changes with ECG signal,
- show examples of in vivo and in vitro 3D reconstructions

The first two items are for validation of temporal synchronization. The following two are to evaluate the spatial positioning accuracy. The fifth item is to prove the need for ECG data for a better reconstruction. Finally, the last item is to demonstrate several possible reconstructions.

12.1 In Vitro Experiments

12.1.1 Setup for In Vitro Experiments

The laboratory setup for in vitro experiments is shown in Figure 36. A computer is connected to the flow generator to choose the flow waveforms and parameters. A liquid that has similar properties to blood is used for blood simulation and pumped by the flow generator through the ends of a flow channel in the flow phantom. The signal generator is loaded with needed waveforms and the output channel of the generator is connected to the ECG input of the ultrasound scanner.

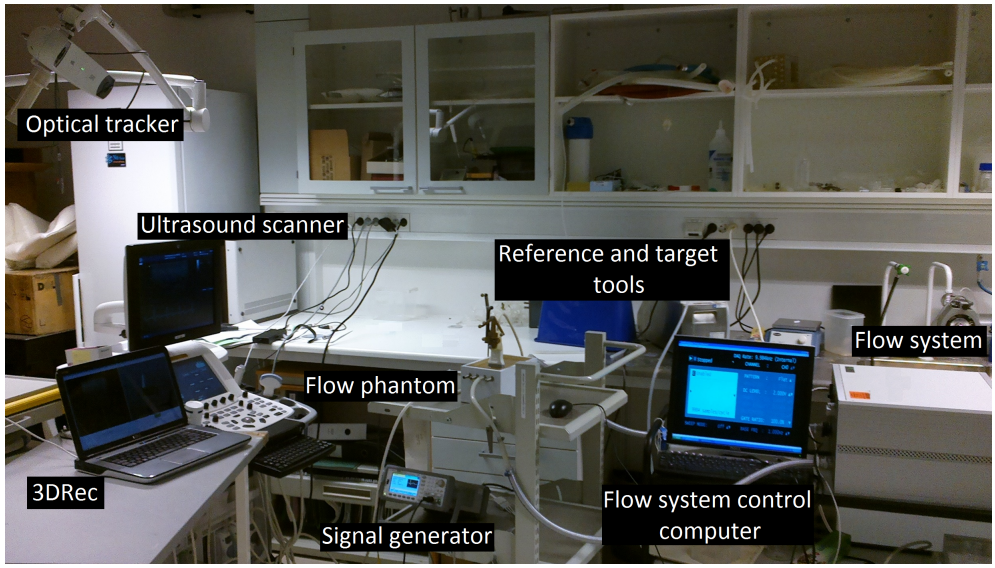

Figure 36: Laboratory setup for in vitro experiments

12.1.2 Peak Detection and Cardiac Cycle Extraction

Recorded ECG signal may be affected by the complex sources of disturbances which cause distortions in the pure ECG signal. Even though the source of the noise is quite complex, the main source is the patient himself [23]. Patient activities such as muscle trembling, patient movement, breathing and sweating introduce noise and make it difficult to analyze the ECG signal [23].

The aim of this test is to evaluate the peak detection and cardiac cycle extraction with perfect and distorted ECG signals. An example of perfect or pure ECG signal is shown in Figure 10. The pure signal that is used for the calculations is created by using MATLAB.

Several different kinds of distortions are introduced to the pure ECG signal by using MATLAB. These distorted signals are then loaded into the signal generator and fed to the ultrasound scanner through the ECG leads. These signals are then captured, synchronized and saved with 3DRec application. Saved data is then analyzed with MATLAB.

12.1.3 Spatial Positioning Accuracy

This test is to evaluate how accurately a slice is positioned in 3D scene. Positioning accuracy is determined by the accuracy of optical tracking system, probe calibration and transformations between the coordinate systems.

The flow phantom that is described in Section 11.3 is used to evaluate the spatial positioning accuracy of the application.

An overview of the method used is depicted in Figure 37. The line L1 in the figure represents an imaginary line going through the center of one of the flow channels (tube) in the flow phantom. B-mode images are acquired along one tube and saved into an .hdf file with synchronized tracking information.

Saved data is imported to MATLAB using `h5read` function. The algorithm explained below is followed for the assessment:

- For each image, find the center of the circle or ellipse (The shape depends on the angle that the image is acquired. Shape is a circle if the probe is perpendicular to the flow tube. Otherwise the shape is an ellipse) in the image manually by obtaining the coordinates of the top, bottom, rightmost and leftmost points of the shapes. This is realized by using `ginput` function which gives the coordinates of the cursor when clicked on the image. The center point corresponds to the point that the image plane and the line L1 intersect.

- Multiply the center coordinates found in the previous step, by tracking matrix that belongs to the image that the coordinates are found from, in order to get the center point coordinates in VTK coordinate system. Note that the found center point coordinates are given by x and y coordinates while the coordinates after multiplication are given by x, y and z coordinates.

- Fit a line to the calculated center points in 3D. This is the line that minimizes the perpendicular distances from the center points to the line. This line corresponds to the line L2 in the Figure 37.

- Find the perpendicular distance from the center point to the line for each image.

The distances, namely the errors are analyzed afterwards. A system without errors would give zero distance for each image. All found center points would correspond to a point on the line L2

The test is performed with and without using a reference tool and results of both tests are then compared with each other. The reference tool is fixed to the flow phantom firmly as shown in Figure 38 to make sure that there is no relative movement between the phantom and the reference tool.

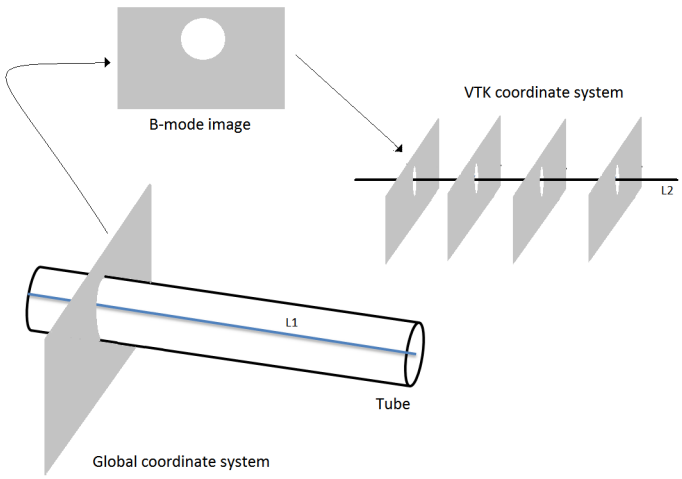

Figure 37: Evaluation test method for spatial positioning accuracy

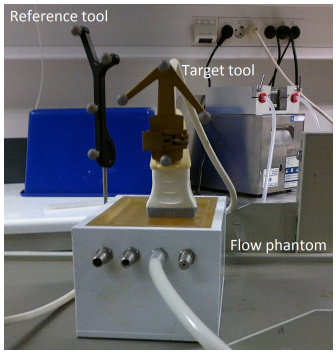

Figure 38: Reference tool placement for in vitro tests

12.2 In Vivo Experiments

12.2.1 Setup for In Vivo Experiments

The setup for in vivo experiments is shown in Figure 39. ECG leads are placed on the patient as explained in section 7.5.1. B-mode image, color flow image and ECG data are streamed from GE Vivid E9 ultrasound scanner and the tracking information is streamed from NDI Polaris Optical Tracking System. A reference tool is fixed to the patient's head for the tests that require a reference tool as shown in Figure 40.

Figure 39: Setup for in vivo experiments

Figure 40: In vivo reference tool placement

12.2.2 Peak Detection and Cardiac Cycle Extraction

Each person is monitored at least one hour and ECG signals are recorded and synchronized with image data by using the application. Images do not have to be informative and there is no need for tracking information since the aim of this test is to analyze the ECG and image data in time axis. Recorded data is analyzed with MATLAB.

12.2.3 Spatial Positioning Accuracy

The carotid arteries of each person is imaged for spatial positioning accuracy tests. 3D reconstruction of an artery is obtained approximately 20 B-mode image slices. In addition, 3D reconstruction of the artery is done with segmentation as explained in Section 10.7.3. Reconstructions are made with and without using a reference tool and results are compared with each other.

12.2.4 Artery Diameter Change During the Cardiac Cycle

This test is to show how the diameter of the artery changes during one cardiac cycle. The objective of the test is to analyze the trend of the diameter change rather than showing the absolute change in mm.

Carotid artery is imaged longitudinally. B-mode images are acquired from the same position for several cardiac cycles. Imaging the artery longitudinally makes it possible to calculate the change from the same point for all cycles (see Figure 41). Information about carotid arteries can be found in Appendix C.

The distance between the walls of the artery is calculated for all images in one cardiac cycle. This is done manually with MATLAB. This is repeated for all recorded cardiac cycles.

Trend of the change is analyzed in order to find out if it correlates well with the ECG signal and to prove that the ECG gating should be included for a better reconstruction.

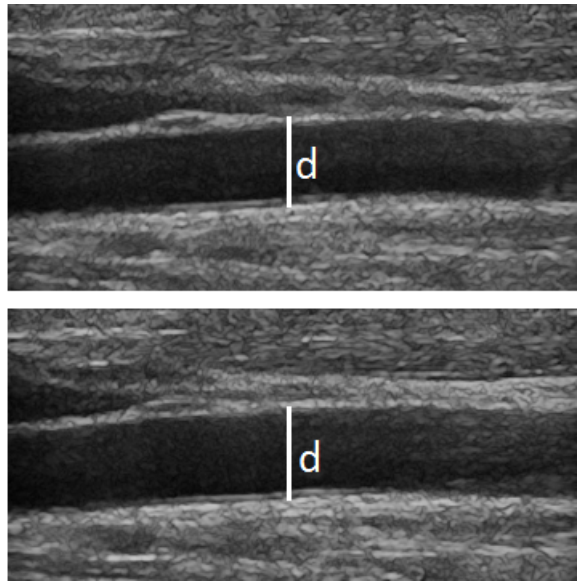

Figure 41: Distance between the walls of artery at its peak (bottom) and lowest (top) length

Part V
Results

This chapter presents the developed 3DRec application and its validation results. First, screen-shots from the application are given to demonstrate the user interface and application features. This is followed by presentation of in vivo and in vitro experiment results.

13 Implementation Results

This section is to present the 3DRec application visually to demonstrate the graphical user interface and the results of implementation methods that are explained in Section 10.

Figure 42 shows the entry point to the application. The user can choose between the modules to start the streaming. Analysis module is an unfinished module and it will be explained in Part VII.

The user can choose if a reference tool will be used for 3D reconstruction. In addition the user can choose the probe type here. Default probe is 11L if nothing is chosen. Even though the application is implemented for using two probe types, it is tested only with 11L probe.

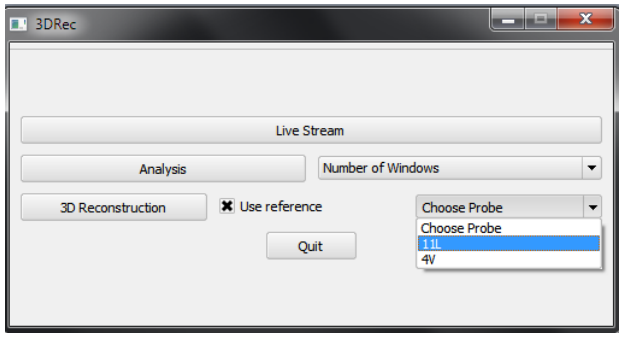

Figure 42: Startup window to choose initialization settings and between the modes

Figure 43 shows the main window of 3D reconstruction module when there is only ECG and B-mode image streaming available.

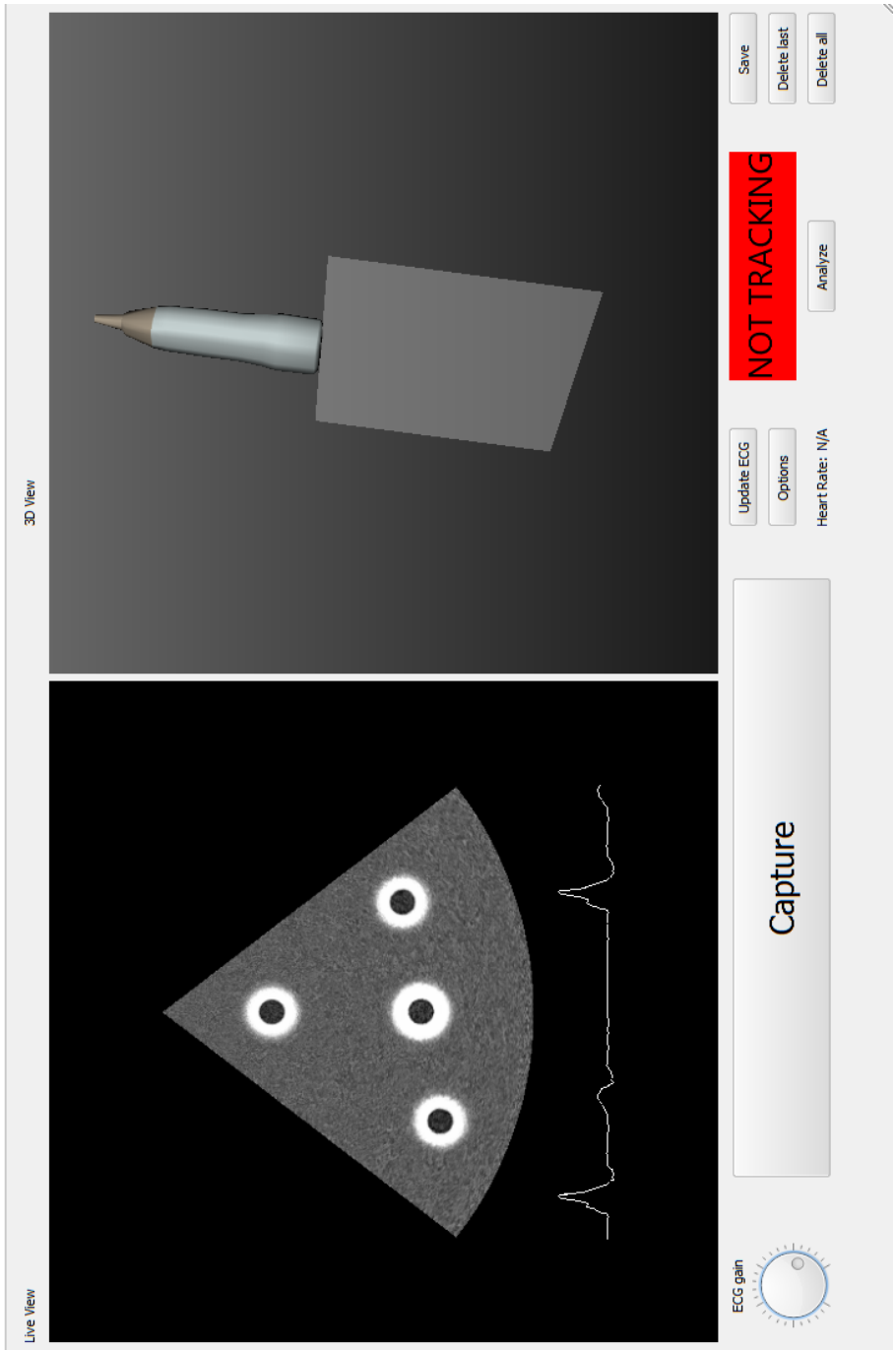

Figure 43: Main window of 3D Reconstruction module with only image and ECG data streaming

Figure 44 shows the status bar and progress bar of the 3D Reconstruction module. Status bar is the way to communicate with the user. It is used to display the notifications. Several notifications are shown in the figure. Also the progress bar (see Section 10.3) of the data capture process is shown in the figure when there is no probe movement during the data capture process.

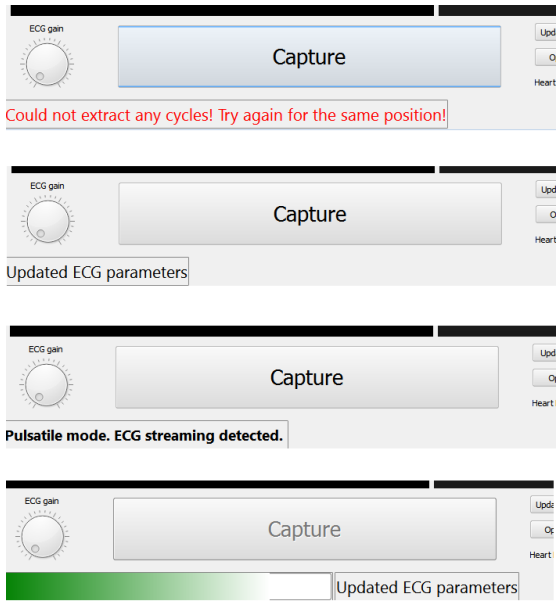

Figure 44: Status bar and progress bar of the main window

Figures 45 and 46 show the analysis window of 3D Reconstruction module. This window can be created by clicking the Analyze button in the main window. If the number of display windows is not chosen, the window will be initialized with two display windows as shown in Figure 45. The user can navigate through the slices with < Previous and Next > buttons. Slider is used for showing the images that belong to one cardiac cycle one by one. Slider changes images in all display windows at the same time. Displayed images in this window are synchronized in time such that all images that are displayed at the same time belong to the same phase of the cardiac cycle. User can replay the captured cardiac cycles by clicking the Play button and save the captured data by clicking the Store button.

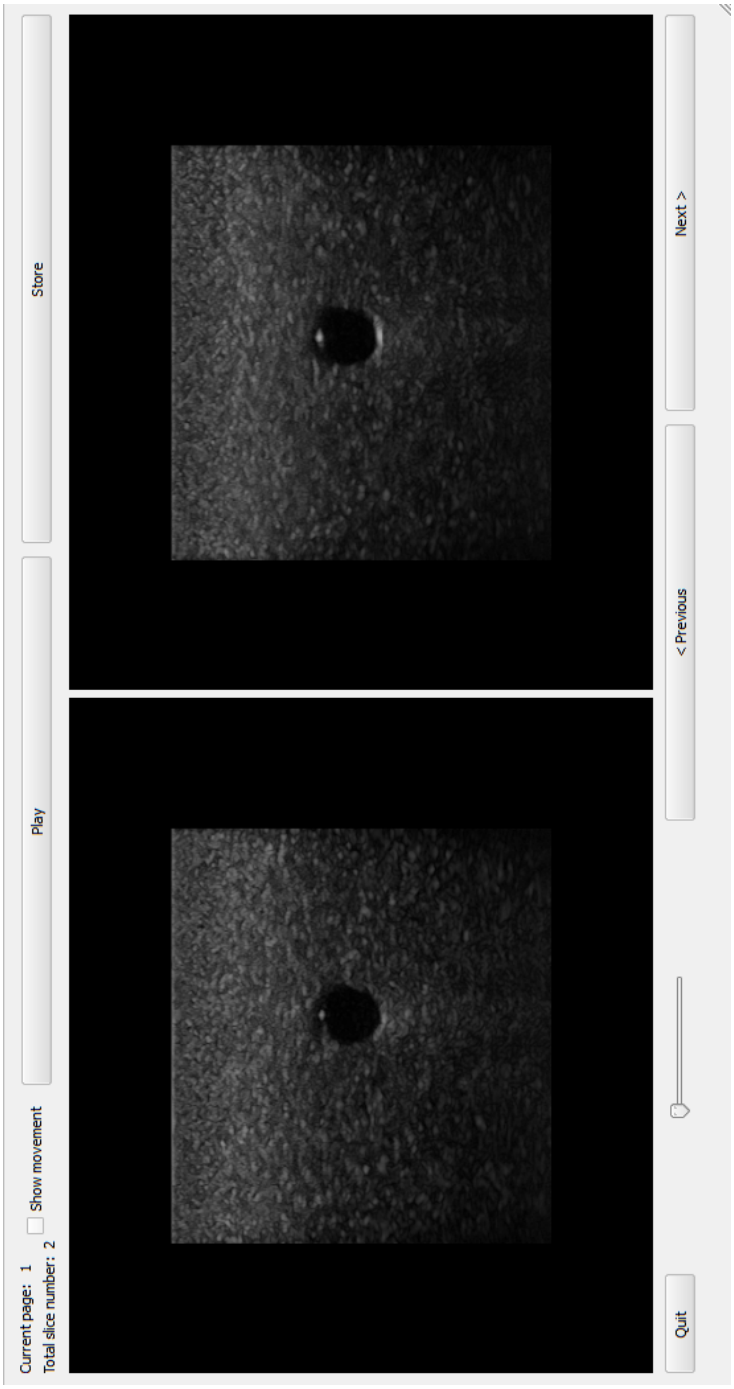

Figure 45: Analysis window of the 3D Reconstruction module with two display windows and show movement disabled

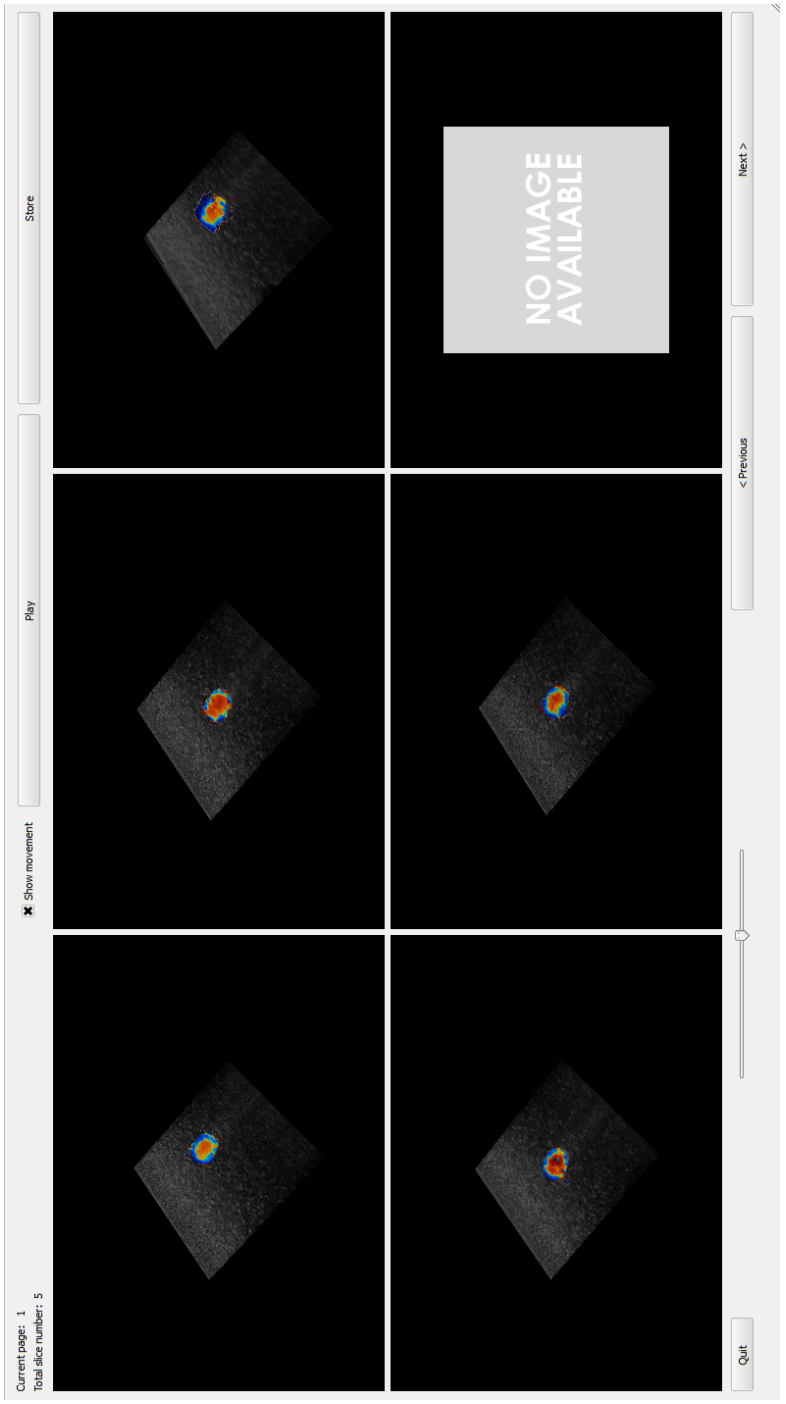

Figure 46: Analysis window of the 3D Reconstruction module with show movement enabled and six display windows

Figure 47 shows the options menu of the main window. This menu becomes visible by clicking the Options button in the main window. The OK button in the menu saves the changes that have been done while the Cancel button discards the changes.

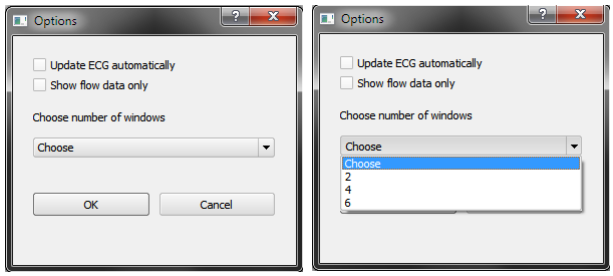

Figure 47: Options menu of 3D Reconstruction module

Figure 48 shows the main window of the Live Stream module of the 3DRec application. This module is chosen by clicking the Live Stream button in the startup window (see Figure 42). This module is used when only streaming of the image and ECG data is desired. Received data is only displayed and cannot be saved.

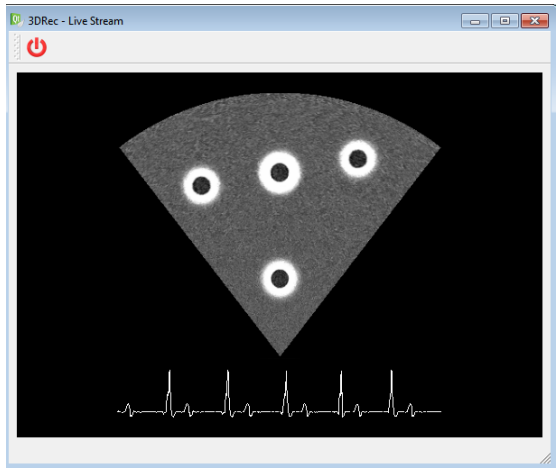

Figure 48: 3DRec Live Stream module

Figure 49 shows the result of temporal calibration test explained in the Section 10.5.1. The test is repeated 30 times to determine a mean temporal shift between the image and the tracking information. The mean time shift is found to be 90.4 ms and the standard deviation is 13 ms. Mean time shift is extracted from the tracking information time stamp to synchronize the image and tracking data.

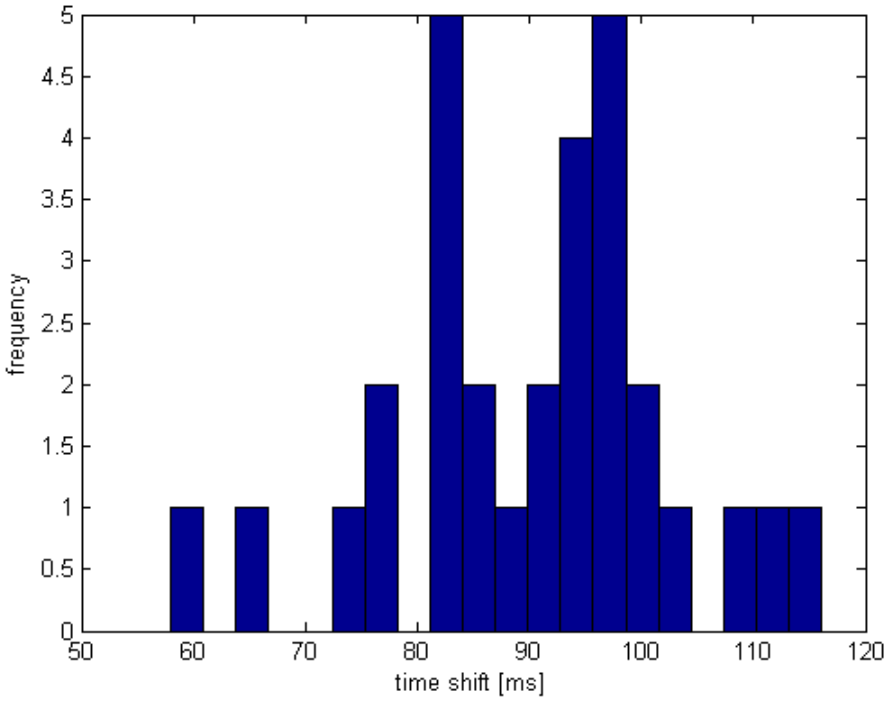

Figure 49: Histogram showing the result of temporal calibration

14 Validation Results

This chapter provides the result of the tests that were performed to evaluate the temporal and spatial accuracy of the 3DRec application.

14.1 Results of In Vitro Experiments

This section presents the result of experiments explained in Section 12.1. Temporal and spatial test results are given separately. All test are performed under the same conditions.

14.1.1 Peak Detection and Cardiac Cycle Extraction Results

Figure 50 presents the result of peak detection and cardiac cycle extraction in case the ECG signal is pure, which means the signal is undistorted. Stripes with circles on top represents the captured images. ECG data and stripes representing the images are plotted together to show where the images belong in the ECG signal. Horizontal axis is the time axis and the position of an image on this axis is determined by its timestamp given on the scanner side. Height of the stripes are always equal to the highest amplitude in the ECG signal and do not indicate any value.

Peak detection and cycle extraction never fails if the ECG signal is pure. Only three different results are given in Figure 50 since all other samples give successfully found peaks and extracted cardiac cycles. Images are always acquired between two consecutive peaks (R points in ECG signal).

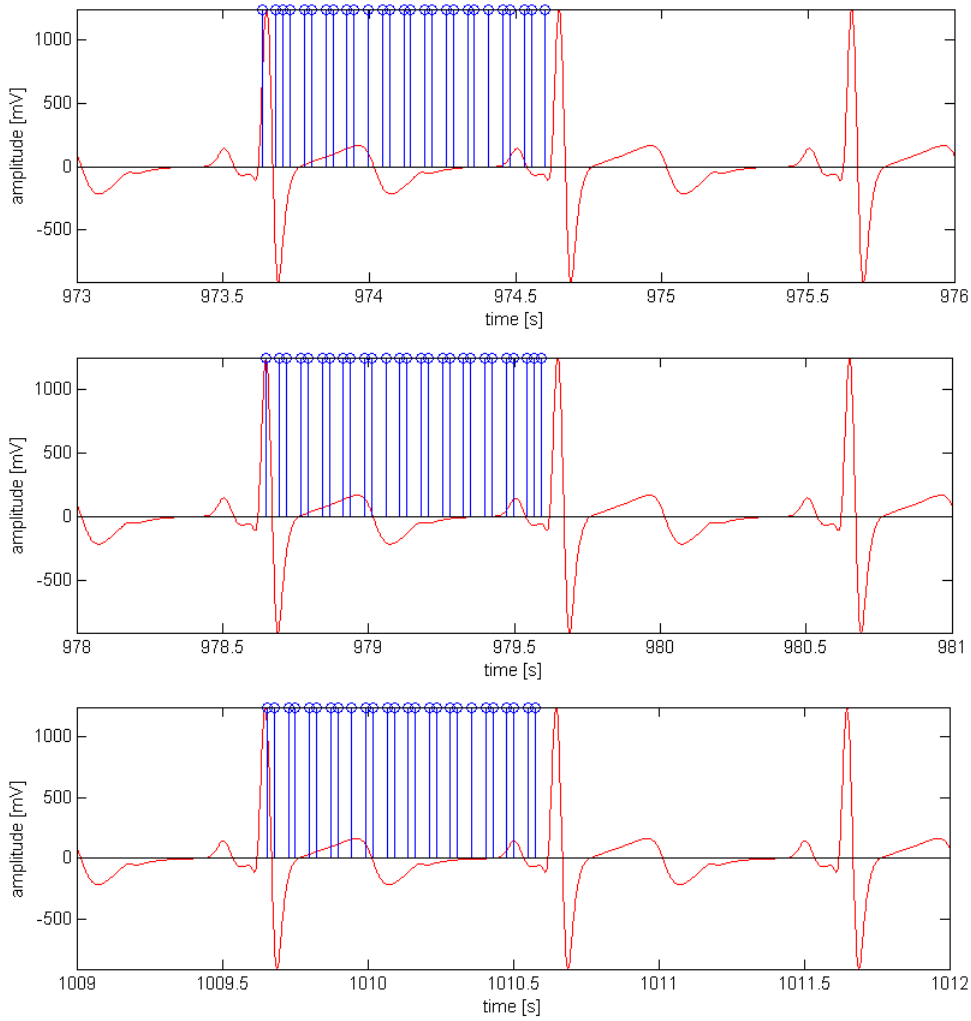

Figure 50: Sample results of peak detection and cardiac cycle extraction test with pure ECG signal

Figure 51 shows the result of a test performed with an ECG signal on which white Gaussian noise is added. Even though a strong noise is introduced to the signal, it is removed by the ultrasound scanner and an ECG signal with a clear peaks was observed.

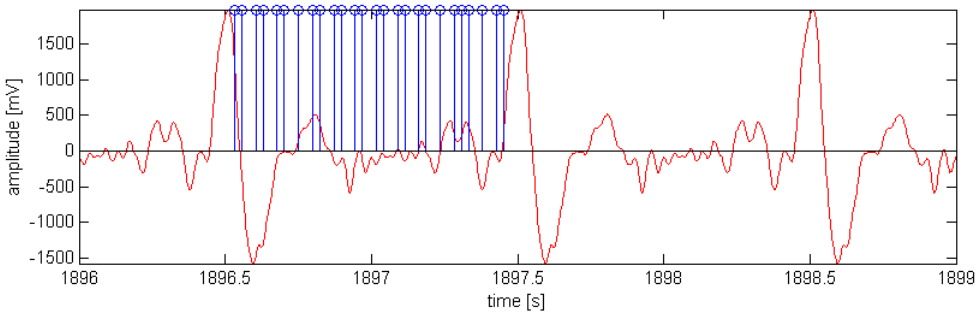

Figure 51: Sample test result of ECG signal with white Gaussian noise

Peak detection and cycle extraction is also tested with ECG signals that have more than one peak in each cycle. Peaks with different amplitudes are added to the ECG signal. Resulting ECG signals and the test results are given in Figure 52. Added peaks have lower amplitudes than the peaks in the original ECG signal. These peaks are located at different positions in the ECG signal.

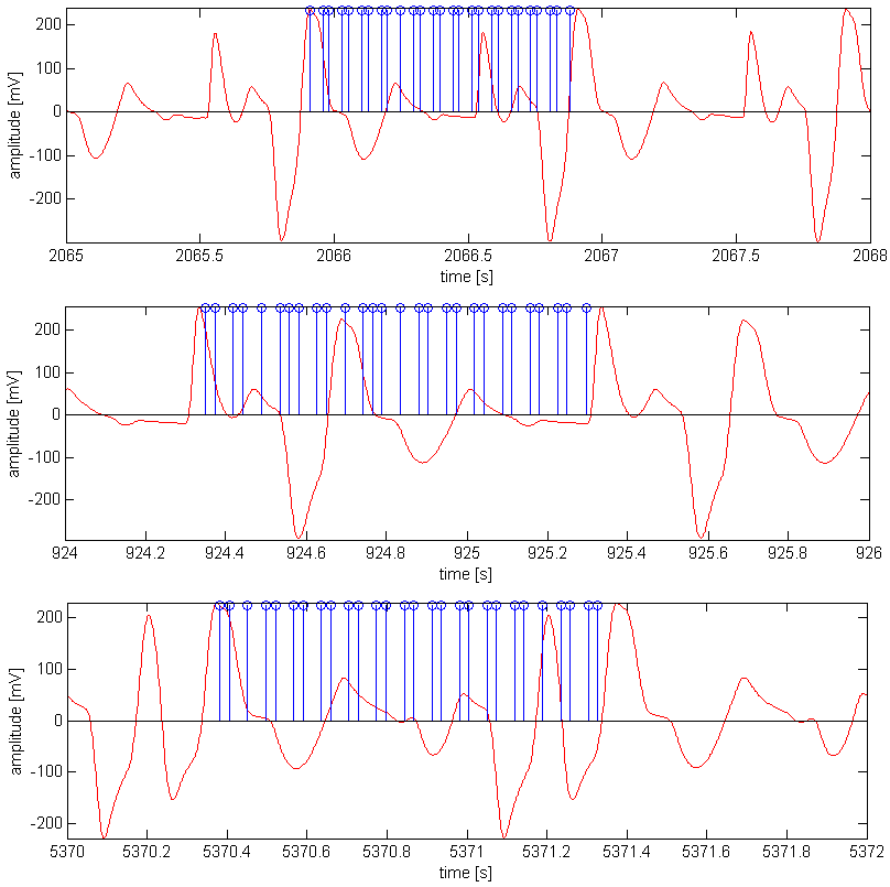

Figure 52: Peak detection and cardiac cycle extraction test results with ECG signals that contain more than one peak in each cycle

To test how peak detection works when changing the ECG signal without updating the ECG parameters, two different signals are used. ECG parameters are first calculated with pure ECG signal that has its peak value at 500 mV. Then, the ECG signal is changed to the signal shown in Figure 53. Two different kinds of failure are observed.

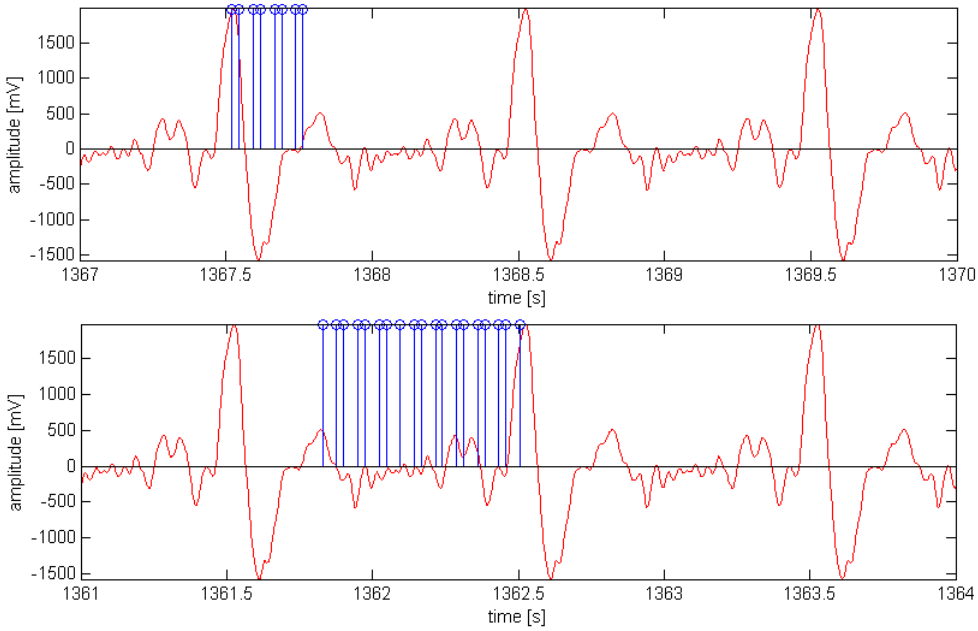

Figure 53: Cardiac cycle extraction failures

14.1.2 Spatial Positioning Accuracy Results

Validation test method for spatial positioning accuracy is explained in Section 12.1.3. Figure 54 shows one example of test result. 2D images are acquired along the flow channel that has 6 mm diameter. The center point of circles/ellipses in 3D are represented by circles in the figure. Coordinates are given in VTK coordinate system.

Figure 55 shows the center points and the line fitted to these data, in VTK coordinate system. This line correspond to line L2 in Figure 37. As can be seen from the figures the center points follow a straight line. The distances between the line and the circles correspond to the instances of total of system error and the errors introduced by the test method used. Errors due to the test method arise from the fact that not the absolute center points are found in the images.

Sub-figures in Figure 56 show the center points in 2D coordinates. The relation between the points is easier to interpret in 2D. The number of circles is equal to the number of 2D images (slices) acquired along the flow channel.

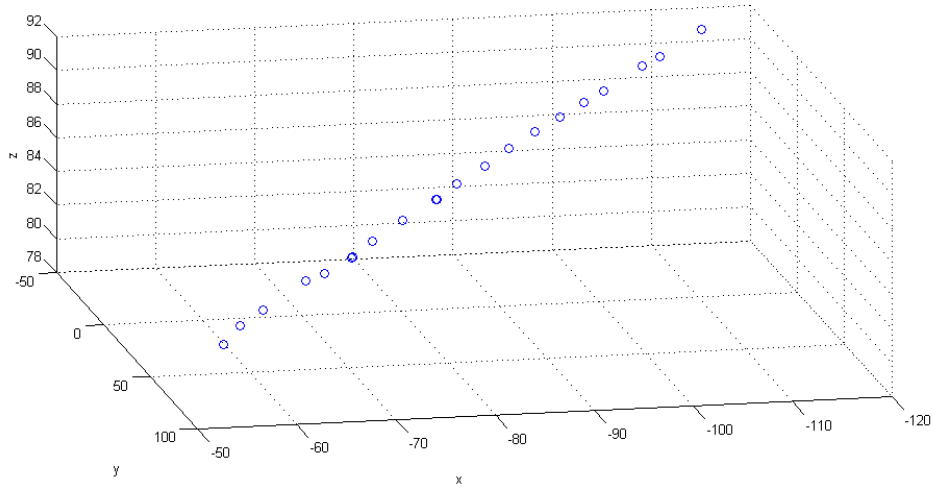

Figure 54: Center points of the circles/ellipses in VTK coordinate system

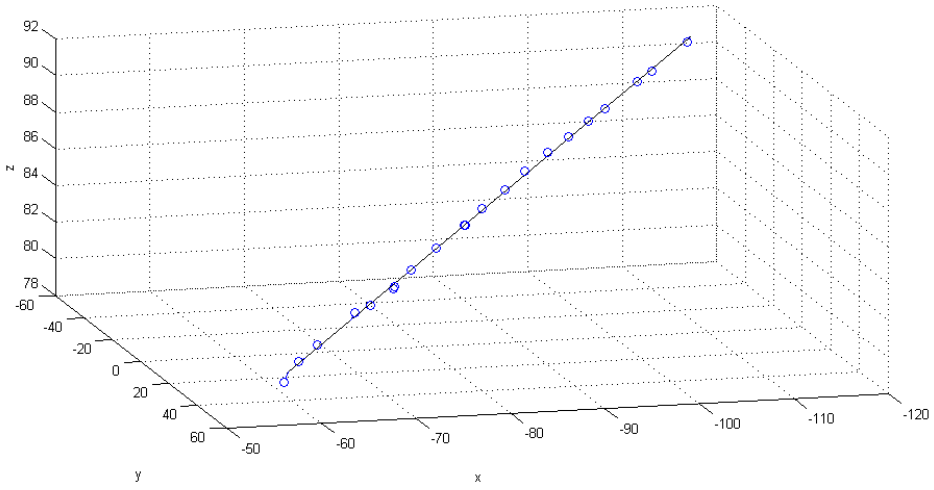

Figure 55: Line fitted to the center points in 3D

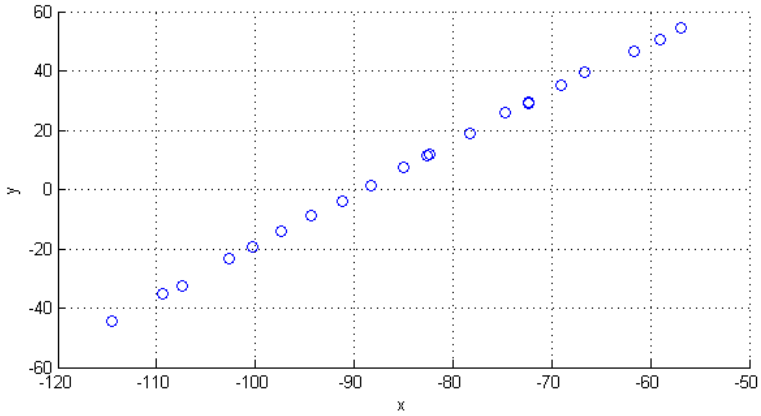

(a) Center points shown by x and y coordinates

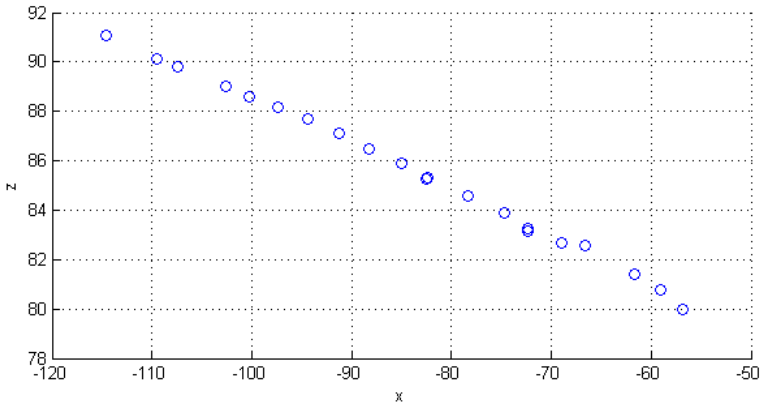

(b) Center points shown by x and z coordinates

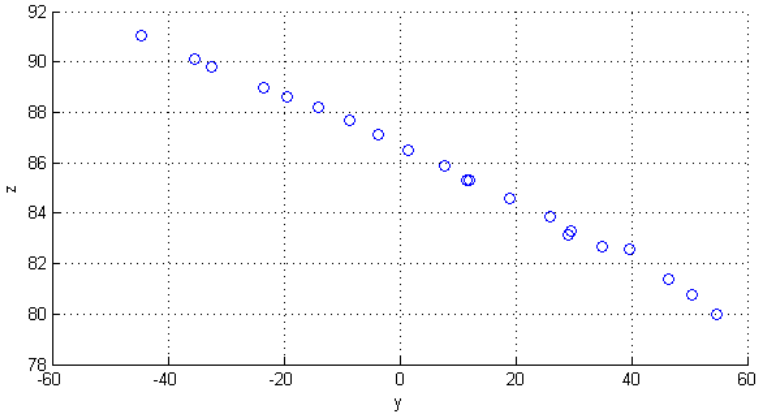

(c) Center points shown by z and y coordinates

Figure 56: Center points shown in 2D coordinates

Sub-figures in Figure 57 show the test results for ten experiments done with 6 mm flow channel. The first histogram shows the result of five tests performed without using a reference tool. Distances are calculated for 97 B-mode images. This results in approximately 20 samples (images) for each test. Namely, about 20 images are acquired from one end to the other end of the flow channel.

The second histogram shows five test results when a reference tool is used. 116 slices are used for calculation in total. This accounts for slightly more than 20 samples per test.

For each five test mean error, standard deviation and root mean square error (RMSE) are calculated. Table 1 summarizes the results of ten experiments.

	Reference tool is not used	Reference tool is used
number of images used	97	116
mean error	0.3665 mm	0.3131 mm
standard deviation	0.2159 mm	0.1859 mm
RMSE	0.4248 mm	0.3637 mm

Table 1: Results of the tests done with 6 mm flow channel

Similarly Figure 58 shows the results for the same experiment done using 4 mm flow channel. The first histogram shows the result of five tests without using a reference tool while the second one shows the result of five tests done using a reference tool. Table 2 summarizes the results of these tests.

	Reference tool is not used	Reference tool is used
number of images used	102	110
mean error	0.3627 mm	0.3026 mm
standard deviation	0.2960 mm	0.2042 mm
RMSE	0.4673 mm	0.3645 mm

Table 2: Results of the tests done with 4 mm flow channel

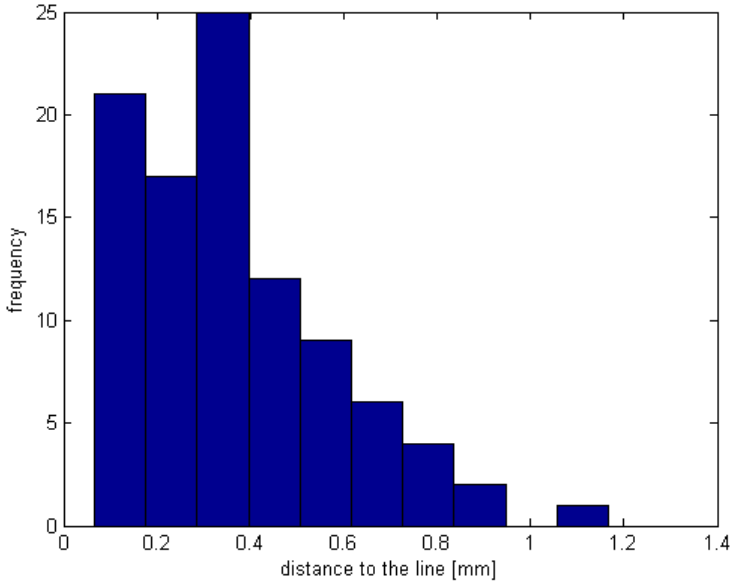

(a) Histogram showing distances from the center points of the circles/ellipes to the fitted line when no reference tool is used.

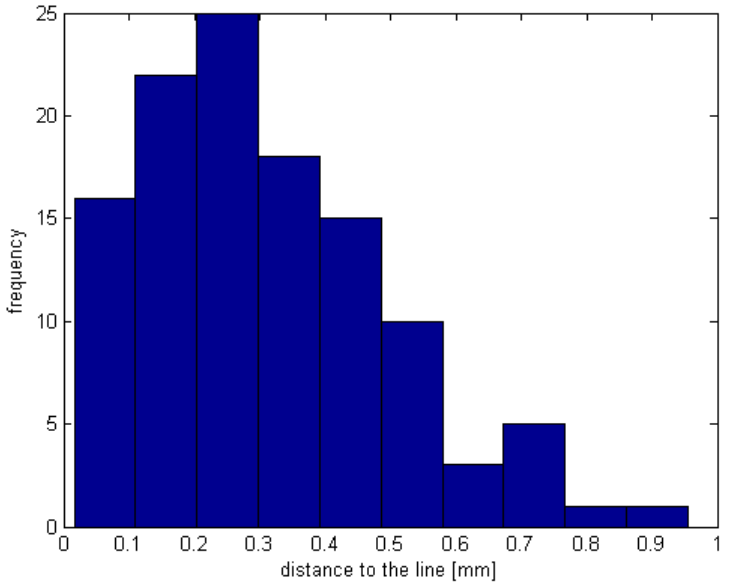

(b) Histogram showing distances from the center points of the circles/ellipes to the fitted line when a reference tool is used.

Figure 57: Histograms showing the spatial positioning accuracy results of experiment done with 6 mm flow channel

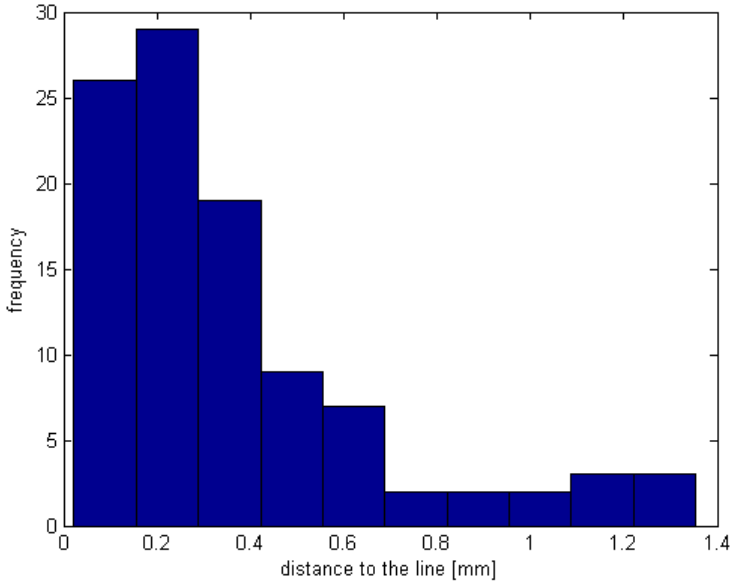

(a) Histogram showing distances from the center points of the circles/ellipes to the fitted line when no reference tool is used.

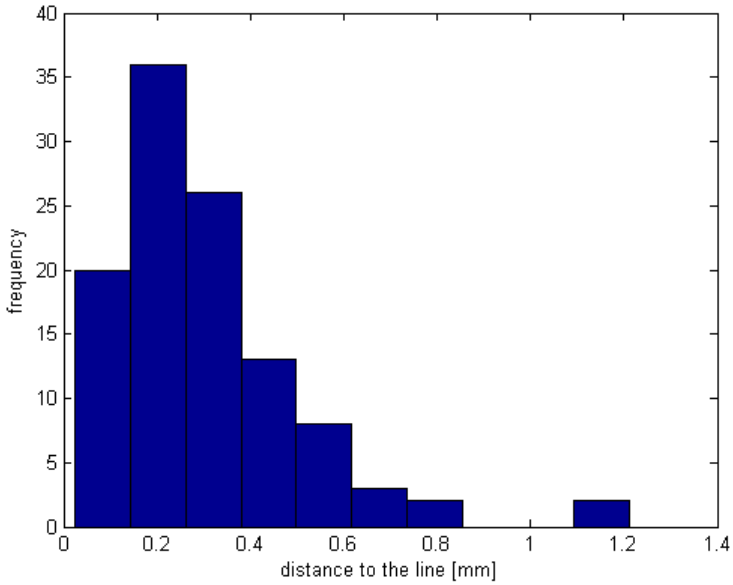

(b) Histogram showing distances from the center points of the circles/ellipes to the fitted line when a reference tool is used.

Figure 58: Spatial positioning accuracy results of experiments done with 4 mm flow channel

Figures 59, 60 and 61 show examples of 3D reconstructions obtained with 3DRec application.

Figure 59 shows three different reconstruction examples. First four images show one reconstruction from different angles. Samples, in this case B-mode images, are approximately parallel to each other and have approximately equal distances in between.

Left bottom image shows a reconstruction with randomly sampled images. Images are not parallel and are not sampled in equal intervals. A line drawn on the top of the image for a better interpretation of the reconstruction.

The reconstruction shown in right bottom image is obtained with equally sampled parallel images but the circles (flow channel cross-sections) are not always in the middle of the image.

Figure 60 shows one 3D reconstruction obtained with color flow images and segmentation. Segmentation is done as explained in Section 10.7.3. The flow channel that has 6 mm diameter is used for the reconstruction. A flat (constant) flow is created with the flow generator. The resulting reconstruction is shown from different angles in the figure.

Finally, Figure 61 shows two B-mode images acquired with 6 mm flow channel. One image shows a longitudinal cross-section of the flow channel while the other one shows a transverse cross-section. These two images are shown from different angles.

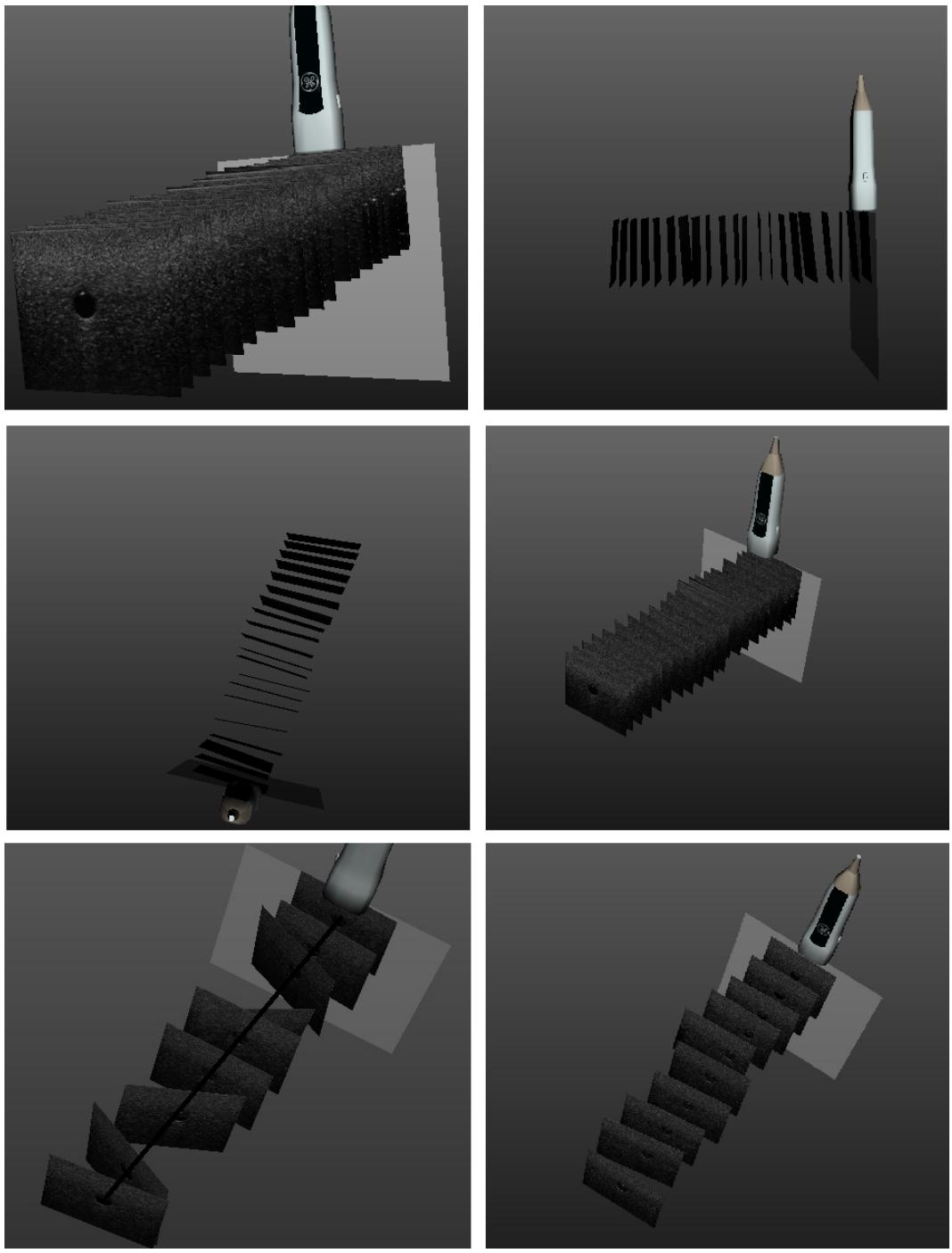

Figure 59: Three different reconstructions obtained with B-mode images

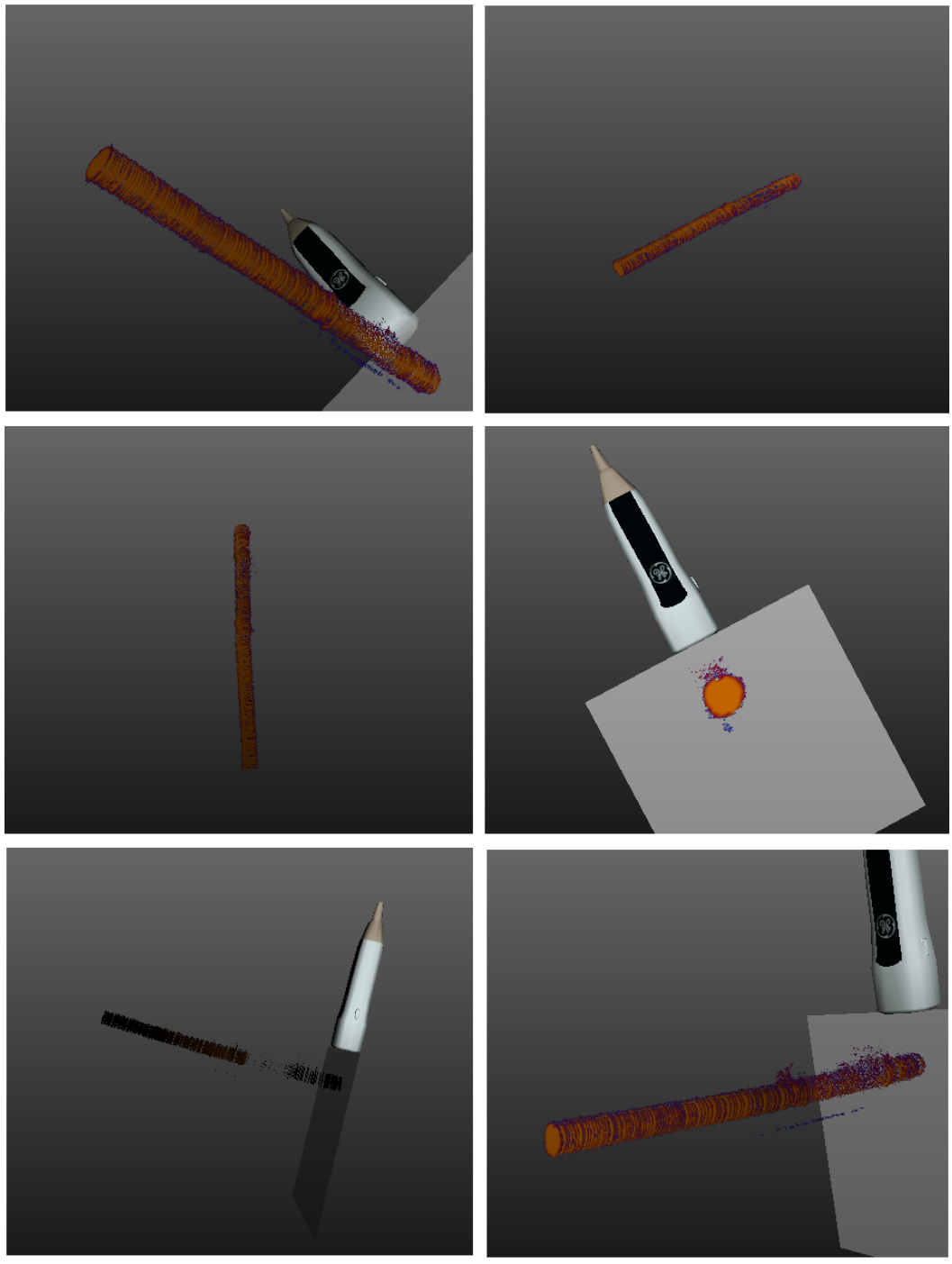

Figure 60: 3D reconstruction obtained with color flow image and segmentation shown from different angles

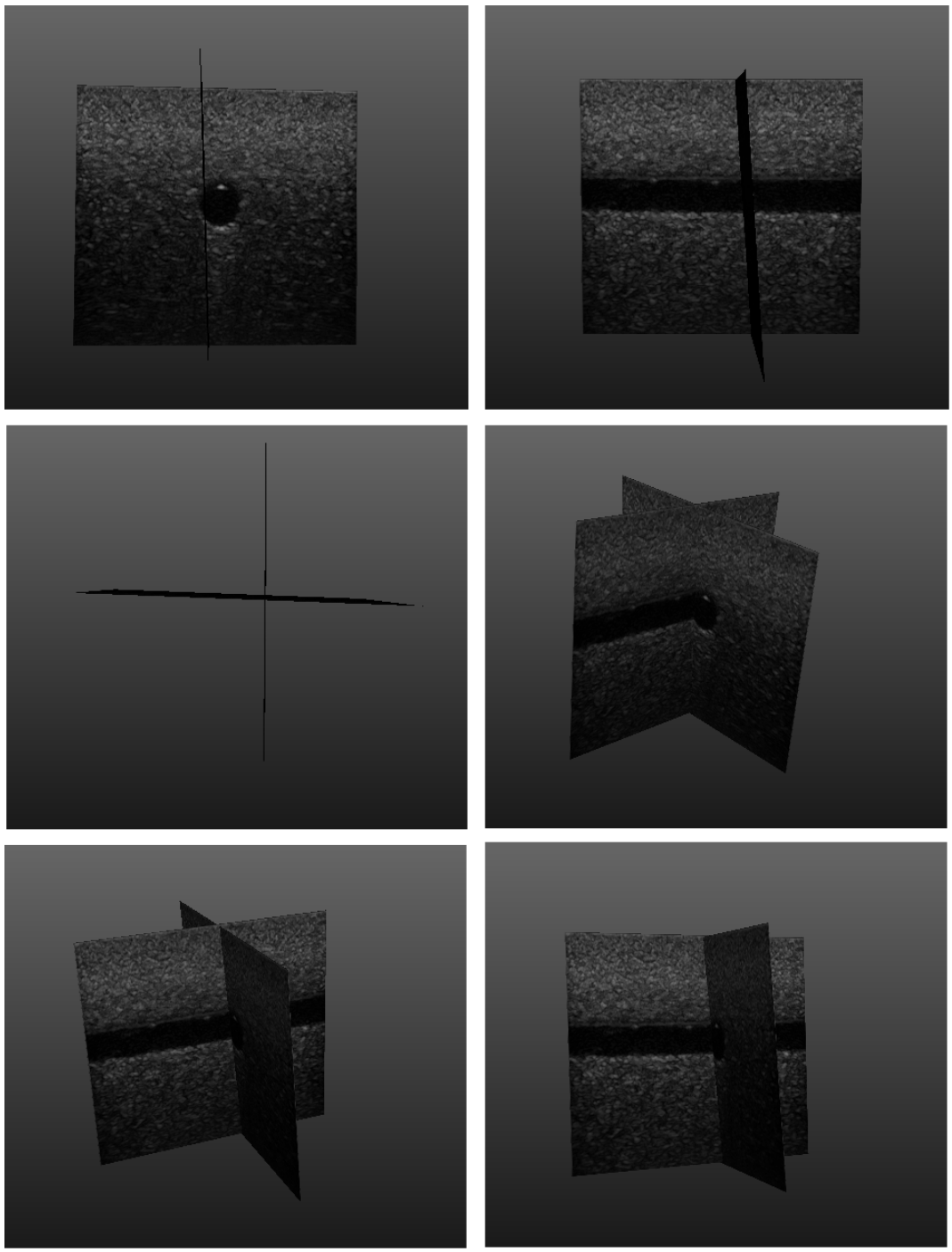

Figure 61: Two approximately perpendicular images acquired from 6 mm flow channel

14.2 Results of In Vivo Experiments

This section presents the results of in vivo experiments. The applied methods for these experiments are explained in Section 12.2.

14.2.1 Peak Detection and Cardiac Cycle Extraction Results

Figure 62 shows ECG samples recorded from three different people. It shows the successful test results for each person. As seen from the figure, last two ECG samples have one peak value in each cycle. Peak detection and cardiac cycle extraction could be performed without any errors for these two people.

In contrast to the two last samples, first ECG sample has two peaks in each cycle and these peaks have quite close amplitudes in all cycles. This results in inaccurate ECG parameter calculation. Interval length can change for each calculation. It can be the interval between R-T, R-R and T-T (see Figure 10) points in the ECG signal depending on the computed threshold value.

Figure 63 shows three different cardiac cycle extraction failures. It is seen that all the found cardiac cycle fall between two peaks even though chosen peaks are not the correct peaks that will give one complete cardiac cycle. Possible reasons of the failures will be discussed in Part VI.

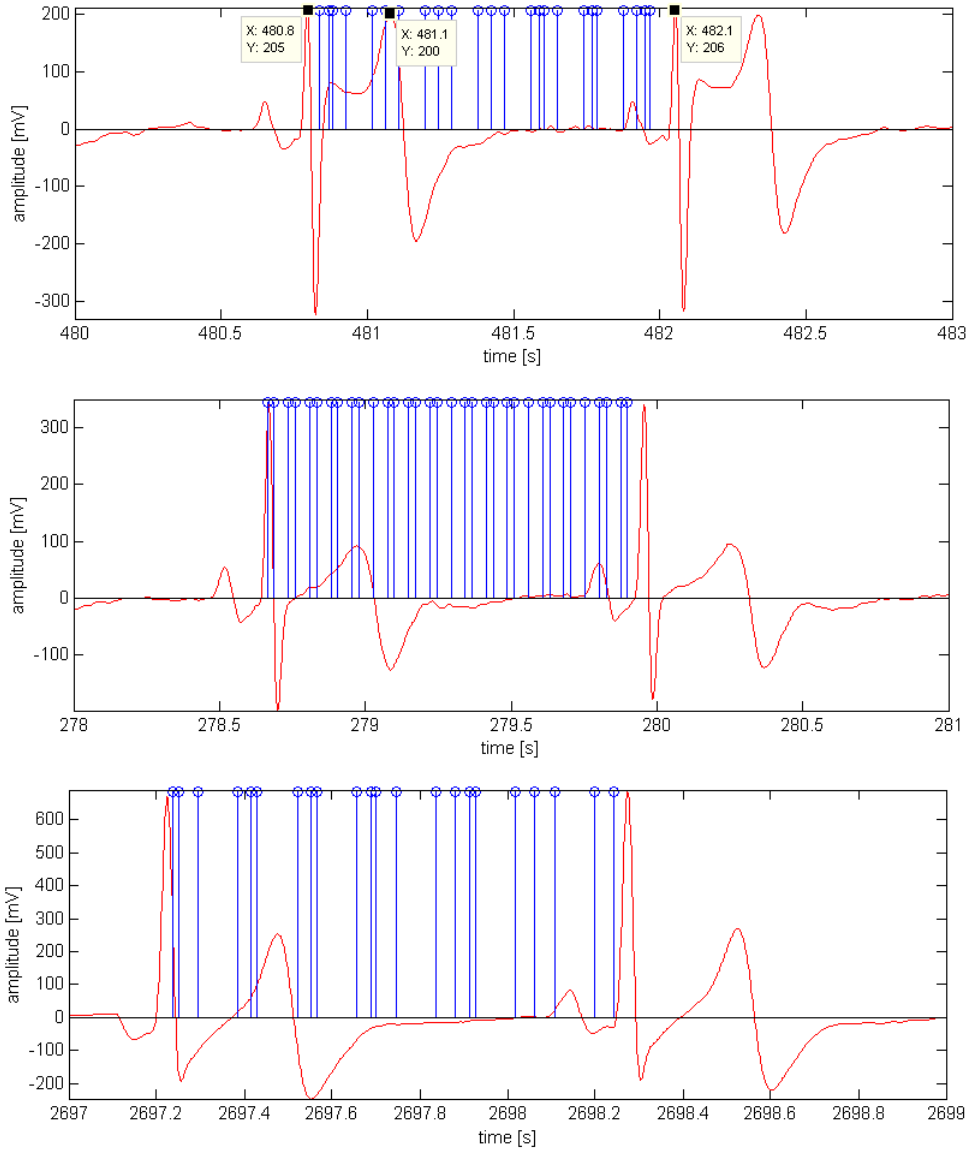

Figure 62: ECG peak detection and cycle extraction results obtained from three different people

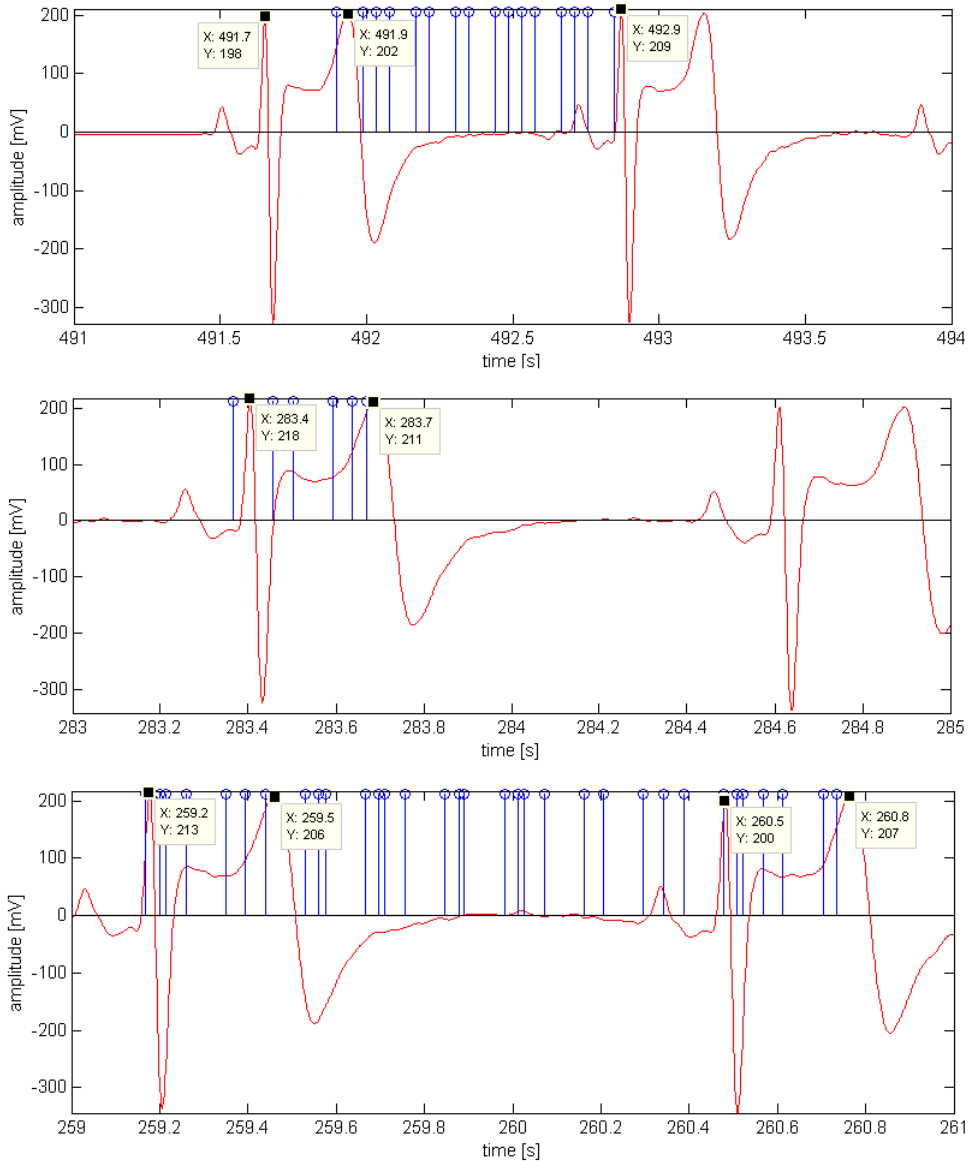

Figure 63: Different types of cardiac cycle extraction failure

14.2.2 Example Reconstructions

This section gives couple of carotid artery reconstructions with B-mode and color flow images. The quality of the reconstructions are highly dependent on the patient movement during the test. Therefore no numerical validation is done based on in vivo images to evaluate the spatial positioning accuracy or to give a system error. In vivo reconstructions are assessed visually by images unlike in vitro experiments.

Figure 64 shows a reconstruction obtained with B-mode images. Continuity of the surrounding area of the artery can be seen in the images.

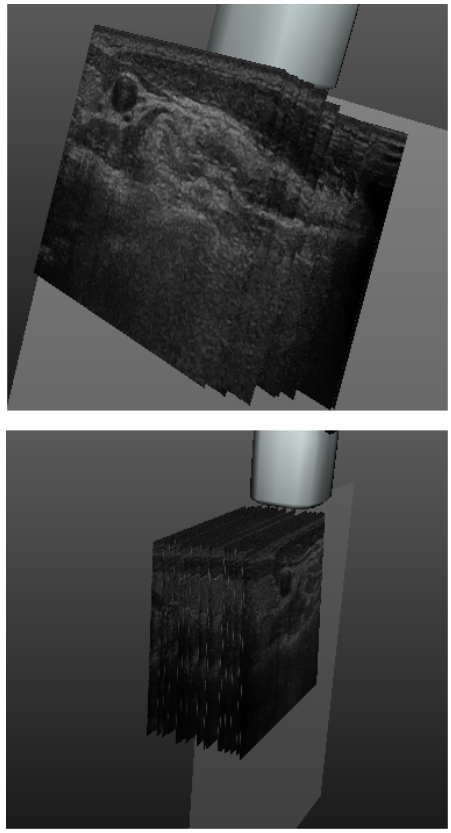

Figure 64: 3D reconstruction of carotid artery with B-mode images

Two approximately perpendicular images are shown in Figure 65. One image shows a longitudinal cross-section of the carotid artery while the other one shows a transverse cross-section. These images are shown from two different angles.

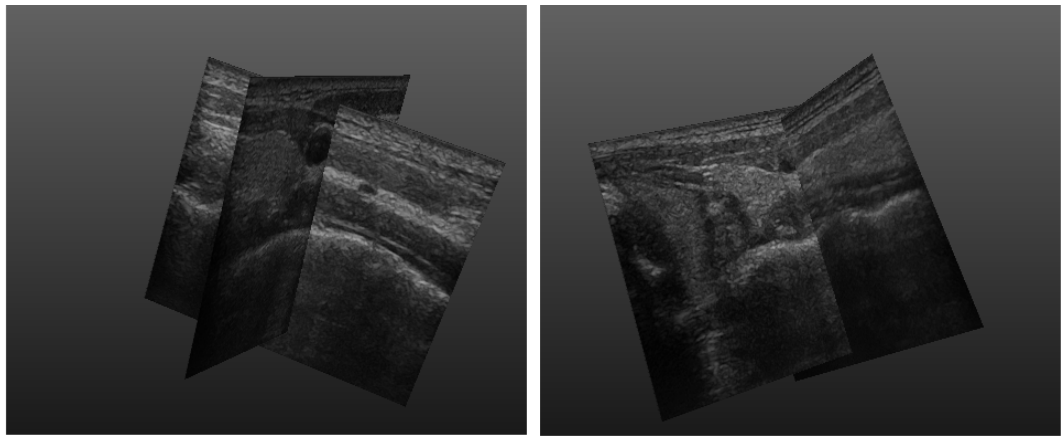

Figure 65: Transverse and longitudinal cross-sections of carotid artery

A 3D reconstruction of carotid artery with color flow images and segmentation is given from different angles in Figure 66. By analyzing the pictures visually, it can be concluded that the person who was being imaged was quite stable during the experiment.

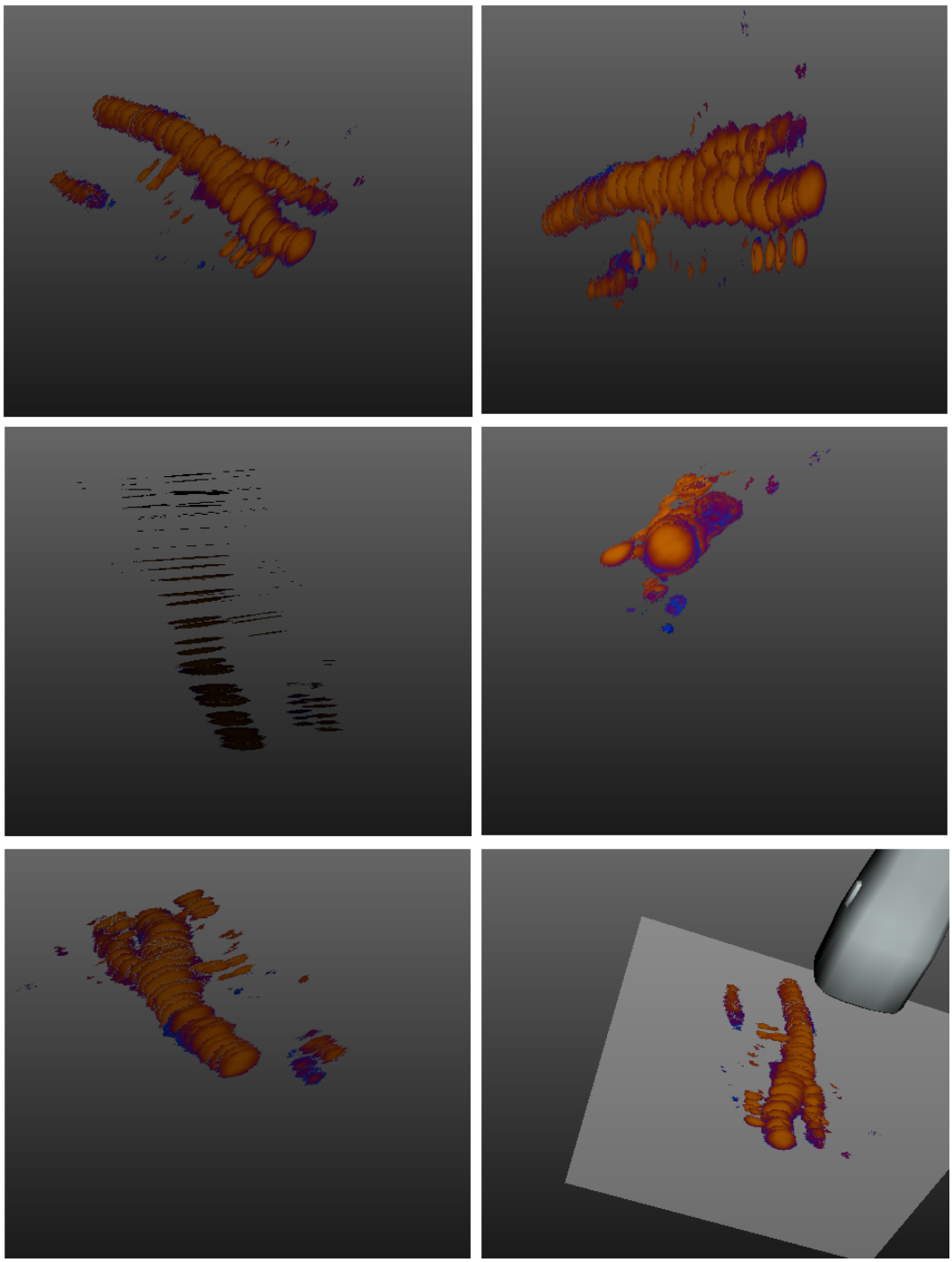

Figure 66: 3D reconstruction of carotid artery with color flow images and segmentation

Figures 67 and 68 show two examples of reconstruction failures due to patient movement. Reconstruction given in Figure 67 is done without using a reference tool. Firstly, images are acquired starting from the black line and towards the direction that arrow 1 is pointing. After acquiring enough samples in the direction of arrow 1, images are acquired starting from the same line towards the arrow 2 direction.

It is easily seen that the patient moved during the test. This movement becomes more obvious when the slices are not taken in a sequence. When samples are analyzed separately as direction 1 and 2, patient movement is not disturbing but still apparent. When all images are analyzed together, disturbance becomes obvious.

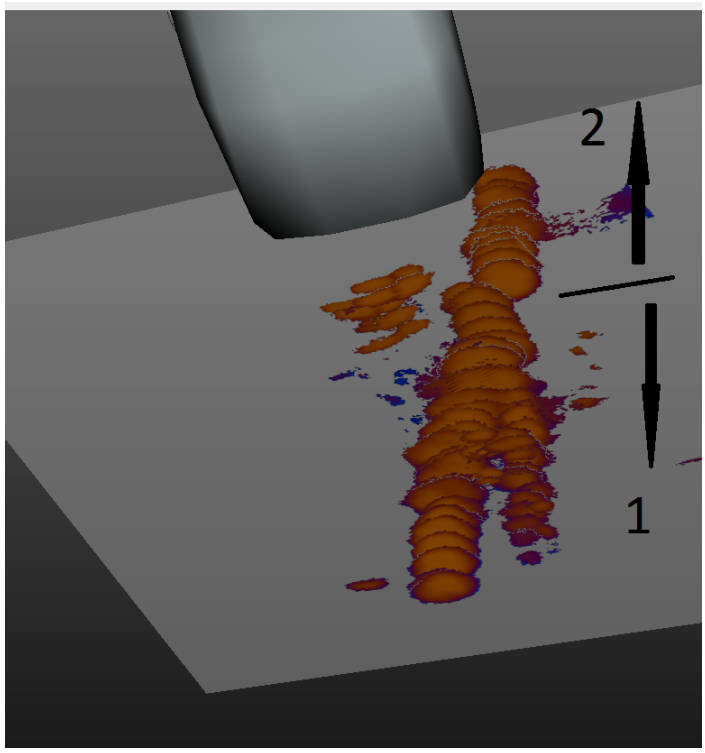

Figure 67: A sample reconstruction done without using a reference tool

Figure 68 shows same kind of failure as in Figure 67. This reconstruction is done by using a reference tool. The movement causes a more severe distortion this time. It may even be interpreted as two different veins even though 2 is continuation of 1.

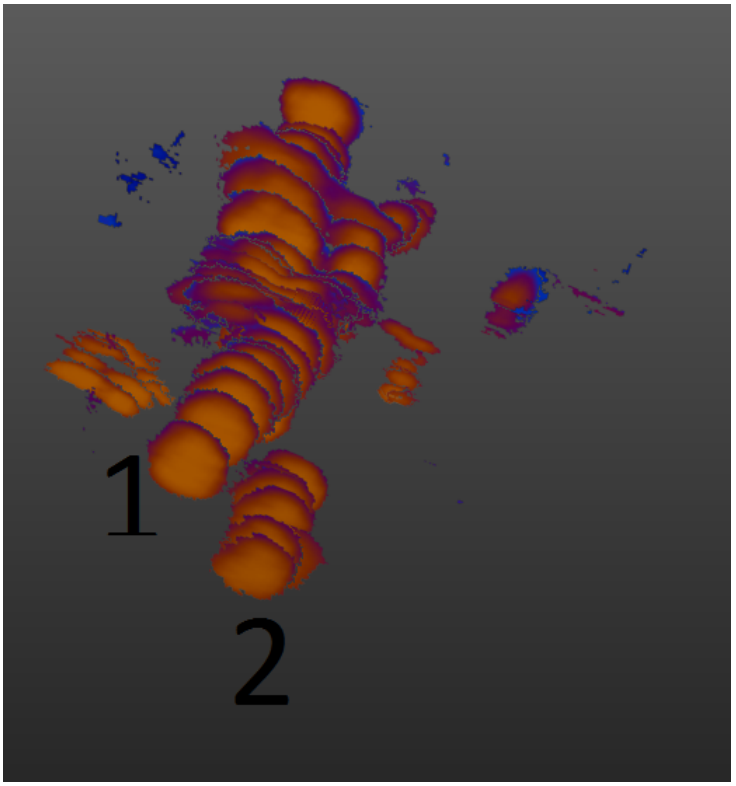

Figure 68: A sample reconstruction done with using a reference tool

14.2.3 Artery Diameter Change During the Cardiac Cycle

Figure 70 shows the changes in the artery diameter for ten different cardiac cycles. It should be noted that these values are not absolute diameters but distances between artery walls at one point in the carotid artery. Section 12.2.4 explains how these distances are measured.

For the sake of brevity, only one ECG signal is given in Figure 69 to show the shape of the signal during one cardiac cycle. This cycle belongs to top left plot in Figure 70. ECG signals belong to the other plots has the same shape as in Figure 69. Slice number correspond to the position of the image that the distance is observed from. One cardiac cycle usually contains around 30 images.

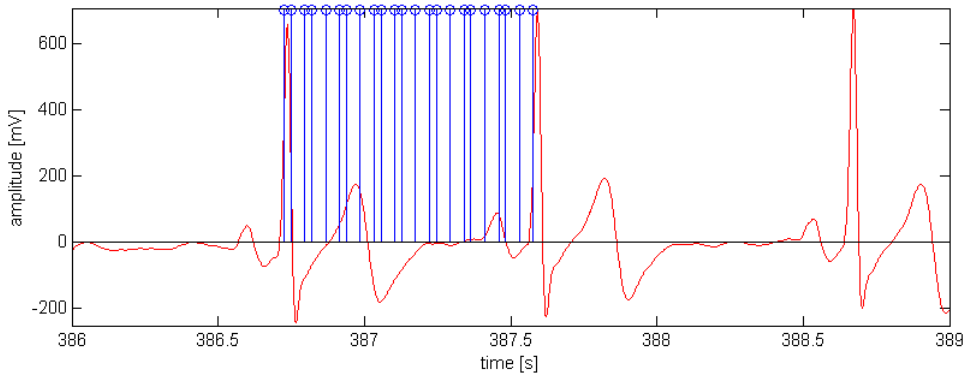

Figure 69: ECG signal belongs to the top left plot in Figure 70

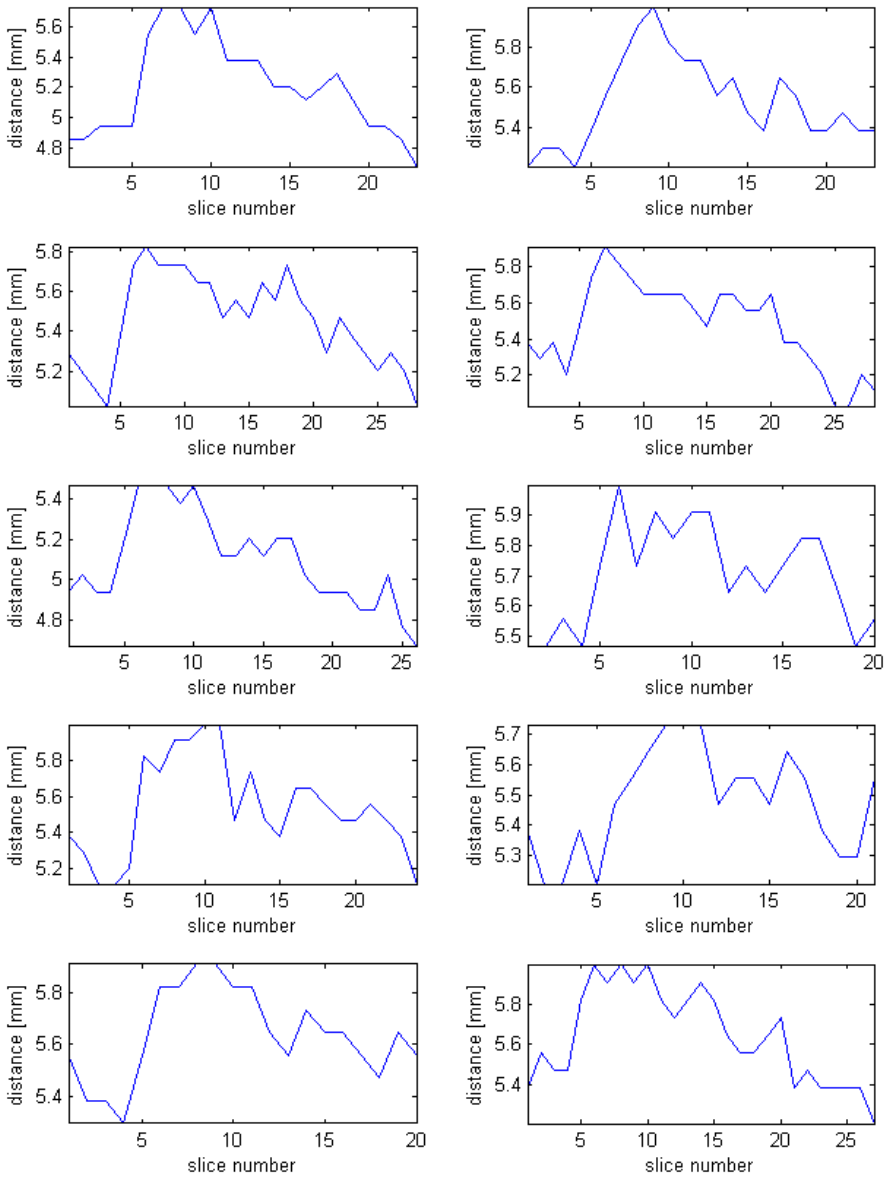

Figure 70: Diameter change during one heart cycle found from one position in the carotid artery

Part VI
Discussion

This chapter gives the interpretation of the in vivo and in vitro test results.

Peak detection and cardiac cycle extraction

By looking at the results of the in vivo and in vitro peak detection and cardiac cycle extraction experiments it can be concluded that the peak detection algorithm do not fail to find peaks in ECG signals that have only one clear peak in each cycle.

It was expected that the ECG signal may have several peaks due to movement or other the sources that cause distortion. Therefore, the algorithm was tested with ECG signals that have more than one peak in a cycle. As shown in Figure 52, in vitro experiments resulted in successful peak detection and cardiac cycle extraction. ECG signals that are used for these tests had peaks that are clearly distinguishable.

Even though the the algorithm never failed to extract the cardiac cycles for in vitro tests, unexpected ECG signals were recorded from a volunteer and the performance of the algorithm decreased considerably during the reconstruction. Error notifications such as “No peaks found” or “Could not extract any cycles” were received. When the recorded data is analyzed with MATLAB it was seen that the main cause of the errors is the T wave that has the amplitude quite close to the R wave. The algorithm assumes that there is only one peak in the ECG signal that is always distinguishably higher than the other values in the signal.

How this situation affects the peak detection and cycle extraction is presented in Figure 63. The first plot shows a cardiac cycle extraction that images that are extracted fall between T and R waves. Even though a threshold that filters the smaller values is computed, chosen peaks do not give a complete cycle as peak values are close to each other. In addition, it is difficult to say if a correct cycle length (interval length in Figure 26) is calculated.

The second plot in the same figure proves that the cycle length is not calculated correctly. It is clear that the interval length is calculated from R-T points in the ECG signal. The 4th step of the peak detection algorithm (see section 10.4.2) states that after the first peak is found, the following values in the interval equal to the half of the cycle length are skipped. The distance between

the found two peaks is less than half of the interval between two consecutive R points in the ECG signal.

The last plot presents a failure in that more than a complete cycle length of images are extracted from the buffer. As the plot shows, amplitude of the second R wave is less than all other peaks in the ECG signal and a threshold that is higher than this amplitude is computed. Occasionally, during the experiment of the volunteer, ECG parameter updates are needed due to peaks that have low amplitude than the threshold.

One way to check the accuracy of the cardiac cycle extraction during the examination is to compare the heart rate displayed on the ultrasound scanner to the one displayed on the computer. Heart rate is calculated from the found interval length on the client side (by the application). The difference between the heart rates for the volunteers that had clear peaks in the ECG signals was about ± 5 beats per minute (bpm) while the difference for the other volunteer was considerably above this value.

Spatial positioning accuracy

As expected, results of in vitro tests that were performed to validate the spatial positioning accuracy proved that using a reference tool attached firmly to the flow phantom improves the accuracy (see Table 1) of the positioning of slices in 3D scene. This is due to the fact that the origin of the global coordinate system, in this case the reference tool coordinate system, is moving with the flow phantom and a point in the phantom keeps its position in the coordinate system even if the phantom is moving. Improvement is observed for both 4 mm and 6 mm measurements.

Using different flow channels did not change the test results considerably. The centers of the flow channel images were found manually as explained earlier. An evaluation of the method is done by calculating the circle center coordinates for the same image for 10 times for 4mm and 6 mm flow channels. The standard deviation for the x and y coordinate changes are given in the table below.

	x coordinates	y coordinates
4 mm flow channel	0,1448 mm	0,0946 mm
6 mm flow channel	0,1105 mm	0,0946 mm

Table 3: Standard deviation of the method used for center calculation

Even though no error calculation is done for in vivo experiments, it was

observed that using a reference tool attached on the head decreases the quality of reconstruction. The reason for that is the place that the reference tool is fixed rather than the relative movement between the head and the tool. Movement of the neck causes a larger translation and rotation factor for the head than it does for the neck itself. The tool's origin is moved differently than the carotid artery in the real world coordinates while for the calculation, this movement is considered as the same.

Artery diameter change

Artery diameter change results correlate well with the change of ECG signal. The change follows the same trend as ECG signal however they are not synchronized. The peak distance between the vessel walls occurs around the 6th and 10th image in the extracted cardiac cycle while the ECG peak time corresponds to the first image. This is equal to approximately 198 ms and 330 ms time delay for 6th and 10th image respectively. Therefore the images that are closest to the peak value of ECG signal, which are also used for the 3D reconstruction, do not correspond to the peak values in distance.

The reason that the distance change do not follow a smooth path is the reading error. The distances are found manually with MATLAB from the saved images. In addition, extracted cardiac cycles do not contain the same number of images and the time interval between the images is not constant.

Standard deviation of all distances that are shown in ten plots in Figure 70 is found as 0.2917 mm. Standard deviation of distances found from the first images, which are used for the reconstruction, is 0.2257 mm. As expected, this shows that the use of ECG data improves the synchronization of images used for 3D reconstruction.

Part VII
Conclusion and Future Work

The main goals of the thesis were to develop a software application that can realize 3D reconstruction of geometry and blood flow of the arteries and to validate it.

The application was developed successfully with several useful features that can facilitate the reconstruction process. The results of the spatial accuracy tests showed that the reconstruction can be done with 0.36 mm RMS accuracy. Also, in vivo test results showed that the placement of the reference tool is important for optimal results.

Using ECG data for synchronization of the images can improve the quality of the reconstruction.

Several possible expansions of the developed application are given below.

The data saved to the hard disk cannot be analyzed with the developed 3DRec application. Programs that can read the .hdf files are needed for analysis. The analysis module can provide a way to access the saved data. The files are saved in .hdf format and there are C++ libraries that provide ways to access the information saved in .hdf files. Saved information can be imported into the application by utilizing these libraries. Once the data is accessed by the analysis module, it is possible to replay and analyze the recorded images.

3D reconstruction realized by the 3DRec is slice based and the result is not a 3D volume data. In other words, reconstruction is individual 2D slices positioned in a 3D scene. It is possible to create a volume data from the acquired 2D images by using existing open source C++ libraries. Different kind of segmentations can be done easily on the constructed volume data. It is also possible to extract slices from different views once the volume data is available.

The peak detection algorithm can be improved by incorporating the heart rate found on the scanner side. GEStreamer library can be expanded by stream of the heart rate information and the heart rate found by the application can be compared to this. User can be notified if the difference is above a certain limit. In addition, streamed heart rate can be used in peak detection as it can give a good approximation of interval length.

References

[1] B. Angelsen and H. Torp. *Ultrasound Imaging- Waves, Signals and Signal Processing in Medical Ultrasonics*, volume 1 and 2. 2000.

[2] C. Askeland, F. Lindseth, J. Lervik Bakeng, O. Solberg, and G. Tangen. Custusx: A research application for image-guided therapy. 05 2011.

[3] Tracy Paul Barill. The six second ecg- chapter 4. `http://www.nursecom.com/ECGprimer.pdf`. Accessed: 18/12/2012.

[4] C.D. Barry, C.P. Allott, N.W. John, P.M. Mellor, P.A. Arundel, D.S. Thomson, and J.C. Waterton. Three-dimensional freehand ultrasound: Image reconstruction and volume analysis. *Ultrasound in Medicine and Biology*, 23(8):1209 – 1224, 1997.

[5] Marcus Bauer, Seraina Caviezel, Alexandra Teynor, Raimund Erbel, Amir A Mahabadi, and Arno Schmidt-Trucksäss. Carotid intima-media thickness as a biomarker of subclinical atherosclerosis. *Swiss Med Wkly*, 142:w13705, 2012.

[6] J. Blanchette and M. Summerfield. *C++ GUI Programming With Qt 4*. Prentice Hall Ptr, 2006.

[7] Paul R. Detmer, Gerard Bashein, Timothy Hodges, Kirk W. Beach, Eric P. Filer, David H. Burns, and D.Eugene Strandness Jr. 3d ultrasonic image feature localization based on magnetic scanhead tracking: In vitro calibration and validation. *Ultrasound in Medicine and Biology*, 20(9):923 – 936, 1994.

[8] Brit Morken Hans J. Alker Jon Bjordal Einar Stranden, Carl-Erik Slagsvold. Three-dimensional ultrasound visualization of peripheral vessels. *VASCULAR IMAGING FOR SURGEONS*, pages 71–80, 1995.

[9] David H. Evans, Jorgen Arendt Jensen, and Michael Bachmann Nielsen. Ultrasonic colour doppler imaging. *Interface Focus*, 2011.

[10] A. Fenster, D. B. Downey, and H. Neale Cardinal. TOPICAL REVIEW: Three-dimensional ultrasound imaging. *Physics in Medicine and Biology*, 46:67–99, May 2001.

[11] Andrew Gee, Richard Prager, Graham Treece, and Laurence Berman. Engineering a freehand 3d ultrasound system. *Pattern Recognition Letters*, 24(4 and 5):757 – 777, 2003.

[12] R. Gill. *The Physics and Technology of Diagnostic Ultrasound: A Practitioner's Guide*. High Frequency Publishing, 2012.

[13] H. Gray, S. Standring, H. Ellis, P. Collins, B.K.B. Berkovitz, and C. Wigley. *Gray's Anatomy Edition: The Anatomical Basis of Clinical Practice*. Elsevier Science Health Science Division, 2005.

[14] J.R. Hampton. *The ECG Made Easy*. Made Easy Series. Elsevier Health Sciences, 1997.

[15] W.R. Hedrick, P.D. David L. Hykes, and D.E. Starchman. *Ultrasound Physics And Instrumentation*. Ultrasound Physics and Instrumentation. Mosby, 2005.

[16] John A. Hossack, Jun S. Ha, and Thilaka S. Sumanaweera. Quantitative free-hand 3d ultrasound imaging based on a modified 1d transducer array. *Proc. SPIE 4325, Medical Imaging 2001: Ultrasonic Imaging and Signal Processing*, 4325:102–112, 2001.

[17] Northern Digital Incl. Passive polaris spectra user guide, March 2011. Revision 5.

[18] Ellisiv B. Johnsen, Stein Harald; Mathiesen. Ultrasound imaging of carotid atherosclerosis in a normal population. the tromso study. *Norsk Epidemiologi 2009*, 19(1):17–28, 2009.

[19] Anthony Landry, J. David Spence, and Aaron Fenster. Measurement of carotid plaque volume by 3-dimensional ultrasound. *Stroke*, 35(4):864–869, 2004.

[20] J. Loscalzo. *Harrison's Cardiovascular Medicine*. McGraw-Hill Companies,Incorporated, 2010.

[21] Joseph Nordqvist. What is atherosclerosis? what causes atherosclerosis? `http://www.medicalnewstoday.com/articles/247837.php`. Accessed: 23 Dec. 2012.

[22] Sasan Partovi, Matthias Loebe, Markus Aschwanden, Thomas Baldi, Kurt A. Jager, Steven B. Feinstein, and Daniel Staub. Contrast-enhanced ultrasound for assessing carotid atherosclerotic plaque lesions. *American Journal of Roentgenology*, 198(1):W13–W19, 2012.

[23] Adam JOSKO Piotr FIGON, Pawel IRZMANSKI. Ecg signal quality improvement techniques. *PRZEGLAD ELEKTROTECHNICZNY*, 04/2013:257–259.

[24] R W Prager, U Z Ijaz, A H Gee, and G M Treece. Three-dimensional ultrasound imaging. *Proceedings of the Institution of Mechanical Engineers, Part H: Journal of Engineering in Medicine*, 224(2):193–223, 2010.

[25] Richard W. Prager, A. H. Gee, L. Berman, Richard Prager, Andrew Gee, Laurence Berman, and Cambridge Cb Pz. Stradx: Real-time acquisition and visualisation of freehand 3d ultrasound. *Medical Image Analysis*, 3:129–140, 1998.

[26] Robert Rohling, Andrew Gee, and Laurence Berman. A comparison of freehand three-dimensional ultrasound reconstruction techniques. *Medical Image Analysis*, 3(4):339 – 359, 1999.

[27] Robert Nicholas Rohling. *3D Freehand Ultrasound: Reconstruction and Spatial Compounding*. PhD thesis, University of Cambridge, 1998.

[28] William J. Schroeder, Kenneth M. Martin, and William E. Lorensen. The design and implementation of an object-oriented toolkit for 3d graphics and visualization, 1996.

[29] K. Kirk Shung. Diagnostic ultrasound: Past, present, and future. *Journal of Medical and Biological Engineering*, 31(6):371–374, 2011.

[30] Thomas L. Szabo. 1 - introduction. In *Diagnostic Ultrasound Imaging*, pages 1 – I. Academic Press, Burlington, 2004.

[31] Thomas L. Szabo. 11 - doppler modes. In *Diagnostic Ultrasound Imaging*, pages 337 – XI. Academic Press, Burlington, 2004.

[32] T. Theoharis. *Graphics and Visualization: Principles and Algorithms*. Ak Peters Series. A K Peters, Limited, 2008.

[33] Frank G. Yanowitz. Introduction to ecg interpretation. `http://ecg.utah.edu/pdf/`, July 2012. Accessed: 05/07/2013.

Part VIII
Appendix

A Circular Buffer

Circular buffer is a fixed-size buffer and can be regarded as the end of the buffer is linked to the beginning of the buffer. When the buffer is full, the oldest element stored in the buffer is overwritten.

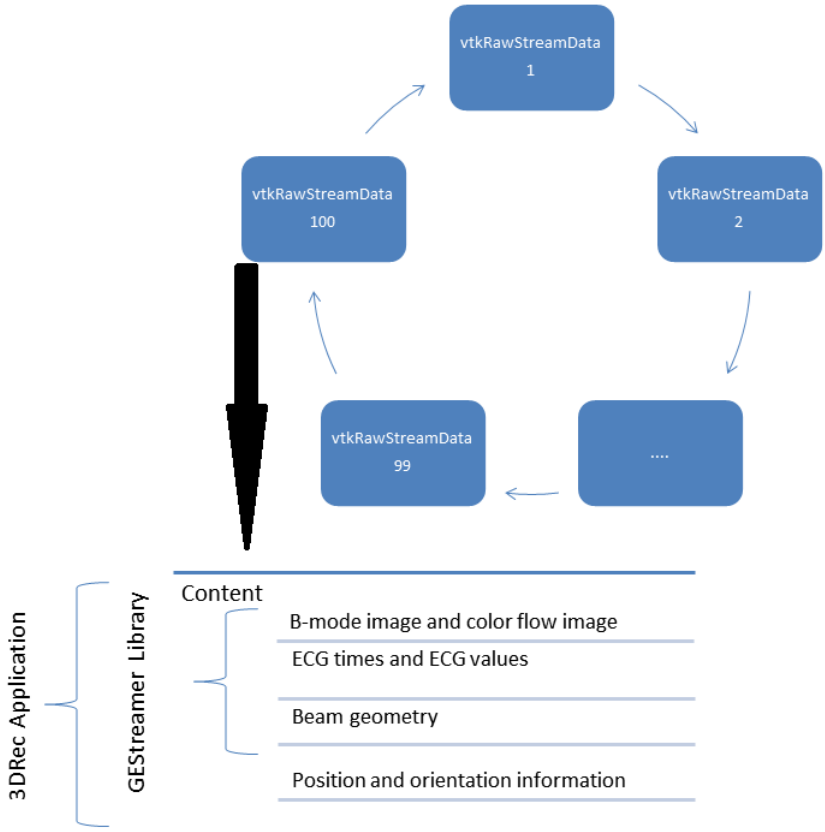

B ECG Update Algorithm

ECG update algorithm

```
1  Initialize start_time to zero
2  for each ECG value and corresponding time stamp{
3
4          if start_time==0
5                  start_time=timestamp
6
7          total_time= start_time - time_stamp
8
9          if total_time < adaptation_time
10                 save ECG value to value_array
11                 save time stamp to time_array
12
13         else
14                 threshold=compute_percentile(value_array,
       percentile_limit)
15                 compute_median_below_treshold()
16
17 }
18
19
20 // Compute threshold for a given percentile rank
21
22 compute_percentile(value_array,percentile_limit){
23 sort saved ECG samples in ascending order
24
25 return the ECG value corresponding to the given
       percentile rank
26 }
27
28 //Compute median time in inervals where ECG signal is
       below threshold
29
30 compute_median_below_treshold(){
31
32 initialize i to zero
```

```
33 initialize N to size of value_array
34
35 while i<N {
36         if value_array[i] < threshold
37                 break
38         else
39                 increase i by one
40 }
41 set in_interval to true
42 set interval_start_time to times_array[i]
43
44 while(i<N){
45         if in_interval is true
46                 if ith element of value_array > threshold
47                         interval_legth = times_array[i]-
       interval_start_time
48                         save interval_length to
       interval_legths_array
49                         set in_interval to false
50         else
51                 if ith element of value_array < threshold
52                         interval_start_time=times_array[i
       ]
53                         set in_interval to true
54
55         increase i by one
56 }
57
58 median_interval_length=compute_percentile(
       interval_lengths_array,50)
59 }
```

percentile_limit in 3DRec application is chosen as 99th. Therefore, threshold is the value that is greater or equal to 99% of the values in three seconds of ECG data.

C The Carotid Arteries

Major source of blood to the head and neck is provided by the common, internal and external carotid arteries [13]. These arteries are located on each side of the neck. The left and right carotid arteries have different origins. Source of the right common carotid artery is the brachiocephalic artery while, on the left, the common carotid artery branches directly from the arch of the aorta [13].

Ultrasound imaging of the carotid arteries can usually be performed without bigger problems as they have a superficial course [5].

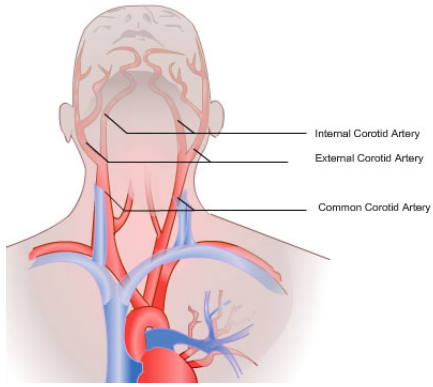

Left and right carotid arteries

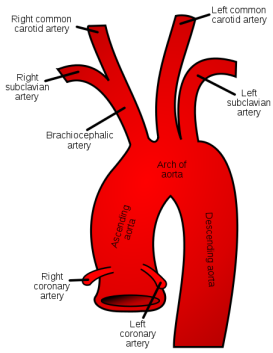

Left and right common artery branching

D 3D Coordinate System Transformations

3D coordinate representations of objects can be transformed from one system to another by a transformation matrix. The procedure explained below yields a transformation matrix M that transforms an object represented in coordinate system A to coordinate system B.

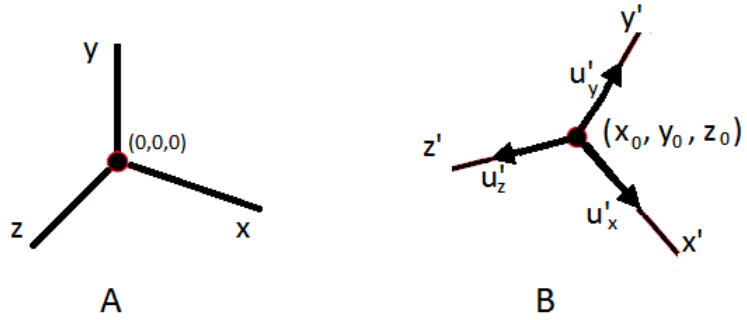

Coordinate system transformation

Firstly, translation transformation is constructed that brings the origin of B to the position of the origin of A.

Translation defines movement by a specified distance in a specified direction [32]. This 3D translation transformation is given in matrix form as

$$\mathrm{T}=\begin{bmatrix}1 & 0 & 0 & -x_0\\ 0 & 1 & 0 & -y_0\\ 0 & 0 & 1 & -z_0\\ 0 & 0 & 0 & 1\end{bmatrix}$$

Next, a rotation matrix that rotates the coordinate system is constructed. The *rotation* transformation rotates an object about the origin. The orientation of the object changes but the distance to the origin stays the same [32]. Rotation matrix that aligns the coordinate systems is given as follows

$$\mathrm{R}=\begin{bmatrix}u'_{x1} & u'_{x2} & u'_{x3} & 0\\ u'_{y1} & u'_{y2} & u'_{y3} & 0\\ u'_{z1} & u'_{z2} & u'_{z3} & 0\\ 0 & 0 & 0 & 1\end{bmatrix}$$

This coordinate rotation matrix transforms the unit vectors $u_x^{'}, u_y^{'}$ and $u_z^{'}$ onto the x, y and z axes respectively.

Then the coordinate system transformation matrix M is given by

$$M = RT$$

Note that if the coordinate systems use different scales, a scaling transformation is also necessary.